Large Timescale Optimization for Communications Over Aerial Ad Hoc Networks With Predetermined Trajectories

Bowen Li, *Graduate Student Member, IEEE*, and Junting Chen, *Member, IEEE*

***Abstract*— This paper studies a delay-tolerant data transportation problem over an aerial ad hoc network where the aerial nodes have predetermined trajectories. The challenge is how to exploit the large-scale channel information predicted from the predetermined trajectories of the aerial nodes to optimize for the communication strategy in a distributive way. The objective is to minimize both the communication energy and the communication time to control the interference leakage to the ground. Most existing approaches for aerial network communications require intensive centralized coordination, but the trajectory information may not be globally available. To tackle these issues, this paper develops a large timescale two-layer optimization strategy using a game theoretical approach. In the inner layer, a mixed timescale optimization on the power allocation and transmission timing is formulated, which is converted into a one-parameter optimization with an optimality guarantee for a deterministic proxy of the original problem. In the outer layer, a *handover time* game is formulated, and a neighbor coordinate response strategy based on local information exchange is developed, demonstrating rapid convergence and near-global optimality in simulations. Numerical experiments demonstrate that, under large timescale optimization, an order of magnitude of cost saving can be achieved.**

***Index Terms*— Aerial ad hoc network, data transportation, caching, delay-tolerant transmission, team strategy, air-to-ground interference.**

Manuscript received 24 October 2023; revised 5 March 2024; accepted 15 April 2024. Date of publication 26 April 2024; date of current version 18 October 2024. The work was supported in part by the National Science Foundation of China (NSFC) under Grant No. 62171398, by the Basic Research Project No. HZQB-KCZYZ-2021067 of Hetao Shenzhen-HK S&T Co-operation Zone, by NSFC Grant No. 62293482, by the Shenzhen Science and Technology Program under Grant No. JCYJ20210324134612033, No. KQTD20200909114730003, and JCYJ20220530143804010, by Guangdong Research Projects No. 2019QN01X895, No. 2017ZT07X152, and No. 2019CX01X104, by the Shenzhen Outstanding Talents Training Fund 202002, by the Guangdong Provincial Key Laboratory of Future Networks of Intelligence (Grant No. 2022B1212010001), by the National Key R&D Program of China with grant No. 2018YFB1800800, and by the Key Area R&D Program of Guangdong Province with grant No. 2018B030338001. An earlier version of this paper was presented in part at the IEEE Global Communications Conference, Rio de Janeiro, Brazil, December 4–8, 2022. The associate editor coordinating the review of this article and approving it for publication was S. Coleri [DOI: 10.1109/GLOBECOM48099.2022.10000858]. *(Corresponding author: Junting Chen.)*

The authors are with the School of Science and Engineering and the Future Network of Intelligence Institute (FNii), The Chinese University of Hong Kong at Shenzhen, Shenzhen Guangdong 518172, China (e-mail: bowenli6@link.cuhk.edu.cn; juntingc@cuhk.edu.cn).

Color versions of one or more figures in this article are available at https://doi.org/10.1109/TCOMM.2024.3393980.

Digital Object Identifier 10.1109/TCOMM.2024.3393980

I. Introduction

LOW-ALTITUDE transportation has been under fast development in recent years. Apart from unmanned aerial vehicle (UAV) sensing and surveillance, UAV cargo transportation for last-mile delivery has proliferated in urban and suburban areas. These UAVs have the potential to form a network that may provide wireless communication support for many emerging applications. One example is data collection in Internet-of-Things (IoT) networks. As many IoT sensors are battery-powered, they prefer short-range and line-of-sight (LOS) communications for energy-efficient transmission [1], [2], [3]. While it is not always feasible to deploy ground base station (BS) close enough to all IoT sensors for short-range and LOS condition, low-altitude UAVs provide a promising solution to the data collection from IoT sensors as it is much easier to establish LOS communication from the air [4], [5], [6], [7], [8], [9], [10], [11].

This paper is motivated by data transportation over a wireless communication network established by these low-altitude UAVs. Such a network has the following characteristics that make it different from conventional communication networks. First, it is a wireless ad hoc network without a reliable network infrastructure, and the network topology is not fixed. Second, as compared to conventional ad hoc networks, the nodes in a UAV network may have predetermined trajectories. For example, the trajectories of cargo delivery UAVs and many patrol surveillance UAVs are determined by the operators before the flight. As a result, it is possible to foresee large-scale communication channels with the aid of channel models or radio maps [12], [13], [14], [15], [16], [17].

Consequently, such a low-altitude aerial ad hoc network gives rise to several new challenges for optimizing the communication strategy. First, it leads to a *large timescale* optimization problem to account for the non-stationary and slow variation of the link quality due to the mobility of the aerial nodes traveling across a long distance. Second, the large timescale network optimization leads to a team decision problem with a *hierarchical information* structure, where the network topology and routing are available globally, but the predicted large-scale channel information is only available *locally*, and the small-scale channel realization is unknown ahead of time. As a result, a team-based mixed-timescale solution structure may need to be developed. Third, evaluating

0090-6778 © 2024 IEEE. Personal use is permitted, but republication/redistribution requires IEEE permission.
See https://www.ieee.org/publications/rights/index.html for more information.

Authorized licensed use limited to: The Chinese University of Hong Kong CUHK(Shenzhen). Downloaded on January 18,2025 at 13:27:52 UTC from IEEE Xplore. Restrictions apply.

and mitigating the impact of air-to-ground interference is difficult. Since the low-altitude aerial node may have a strong channel with a large number of ground nodes, it may interfere with many ground devices. In addition, it is challenging to acquire the geographical positions and channels of the ground nodes being affected due to the nature of ad hoc networks, and hence, it is challenging to design dedicated interference mitigation strategies. One promising solution is minimizing both the transmission energy and transmission time of the aerial nodes. However, minimizing the latter leads to an *on-off optimization* problem that is mathematically challenging to solve.

Most existing works on UAV-assisted communications and data collection have focused on a joint design of the communication strategy and the UAV trajectories. For example, works [15] and [16] considered the mission completion time or the age of information (AoI) to ensure data freshness. Works [17] and [18] adjusted UAV location based on source-destination pairs to maximize the relay throughput. Works [19] and [20] maximized the minimum throughput among all users in an area to ensure communication fairness. Work [21] developed the UAV as a cloudlet to mitigate the computing burden on the edge areas. However, these approaches focus on single UAV deployment, which limits their service range. In addition, these approaches may not be suitable for scenarios where wireless data transportation is merely a side task of the UAV team. For instance, the works in [15], [16], [17], and [18] did not consider the air-to-ground interference, and the data transportation deadline was not guaranteed in [19], [20], and [21].

To extend the service range, works [22], [23], and [24] employed multiple UAVs to enhance coverage. However, these UAVs operate independently and do not interact with each other, leading to poor performance when the source-to-destination distance is long [25]. Works [26], [27], [28], and [29] considered the cooperation among UAVs and exploited channel state information (CSI) and queue state information (QSI) to design transmission strategies. These methods are primarily based on the present and past CSI and QSI. When the realizations or statistics of future CSI and QSI are available, Markov decision process (MDP) and reinforcement learning approaches can be applied [28], [29], [30], [31]. However, these approaches mostly require global information sharing and centralized coordination among UAVs. In addition, the computational complexity substantially increases when the number of network states increases.

In this paper, we address the issue of interference leakage during data transmission in aerial ad hoc networks. The problem is to optimize for the large timescale transmission strategy for the aerial nodes by exploiting the information of their predetermined trajectories via local coordinations. Towards this end, two main technical challenges are needed to be addressed:

- *How to efficiently coordinate the transmissions over a large timescale among aerial nodes based on local information exchange?* Note that global coordination among aerial nodes may not be practical because of the significant signaling overhead and the dynamic nature of the aerial ad hoc network. In addition, the impact of small-scale fading also needs to be handled.
- *How to minimize both the transmission energy and the transmission time for reducing the potential air-to-ground interference?* This leads an on-off optimization problem which is challenging to solve. Note that reducing the transmission time not only saves the circuit power, since the device can be switched to a sleep mode when no transmission occurs, but also reduces the chance of interfering with terrestrial communications, where the channel state information of the ground nodes is hardly available to the aerial network for interference mitigation.

The conference version of this work [32] focused on the local coordination challenge.

To tackle these challenges, we develop a large timescale two-layer optimization strategy using a game theoretical approach. First, we develop a proxy problem to handle the impact from the small-scale fading. While numerous research have performed communication optimization and resource management and control, such as [11], [33], and [34], there is no systematic method to exploit the future channel information efficiently for the optimization of the communication strategy. Then, we use radio maps or channel models to look ahead for the large-scale channel information for the links between adjacent aerial nodes based on the trajectory information. As a result, in the inner layer, we develop a *cache-and-pass* strategy for the minimization of the transmission energy and time; in the outer layer, we optimize for the transmission *handover time* based on local information exchange. Mathematically, we make the following contributions under such a design framework:

- In the inner layer, we develop a mixed timescale transmission strategy to handle the uncertainty due to the small-scale fading, and theoretically prove that the best power allocation and transmission timing can be constructed using a thresholding proxy policy, leading to the development of an efficient algorithm.
- In the outer layer, we formulate the handover time problem using a game theoretical approach, and prove that the Nash equilibriums (NEs) of the game are stationary points of the original problem. Based on these, we develop a distributive mechanism for handover time coordination among aerial nodes, which is shown to converge faster than a conventional coordination mechanism.
- Our simulation results confirm that the proposed mixed timescale transmission strategy and game-based distributive mechanism achieve almost global optimality. The proposed game-based handover time coordination strategy demonstrates a substantially better performance guarantee over conventional schemes also exploiting the trajectory information.

The rest of the paper is organized as follows. Section II presents the decentralized relay transmission model and the problem formulation. Section III develops the mixed timescale transmission strategy. In Section IV, we develop a large timescale team decision strategy to optimize the handover time

Authorized licensed use limited to: The Chinese University of Hong Kong CUHK(Shenzhen). Downloaded on January 18,2025 at 13:27:52 UTC from IEEE Xplore. Restrictions apply.

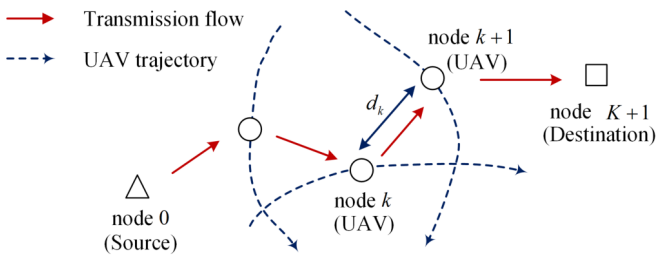

Fig. 1. Illustration of the data transportation scenario where multiple aerial nodes establish the relay path between a source node and a destination node.

parameters. Numerical results are demonstrated in Section V, and conclusions are given in Section VI.

II. System Model

Consider a group of K aerial nodes that follow a set of preset and fixed courses to fly over an area, where a source node on the ground needs to transmit some data to a destination node at a distance. Consider exploiting the aerial nodes to relay the data from the source node to the destination node, as illustrated in Fig. 1. The total amount of data is S bits, and the tolerable end-to-end delay is T seconds. The aerial nodes operate at half-duplex mode, and the transmission order is fixed. In this paper, we assume the transmission order has been configured by the upper-level which takes into account the chronological order that the aerial nodes enter the target area, by the general routing methods, such as contact graph routing (CGR) framework [35]; however, the design of such a protocol is out of the scope of this paper. Without loss of generality (w.l.o.g.), we assume the source node first transmits to the first aerial node, which relays the message to the second aerial node, and so on; finally, the Kth aerial node relays the data to the destination node.

Denote the position of node k at time t as $\mathbf{x}_k(t)$. Here, we assume each aerial node k only knows the trajectories of its own and its neighbors, *i.e.*, node $k-1$ and node $k+1$. This paper aims to design a decentralized transmission strategy for the team of aerial nodes to minimize both transmission energy and transmission time based on *local* information and coordination.

A. Channel Model

The channel gain $\hat{g}_k(t)$ from the kth node to the $(k+1)$th node is modeled as

$$\hat{g}_k(t) = g_k(t)\,\xi \tag{1}$$

where $g_k(t)$ captures the large-scale channel gain and ξ is a random variable with mean $\mathbb{E}\{\xi\} = 1$ to capture the small-scale fading.

Assume that the statistical information of ξ is known ahead of time and the large-scale channel gain can be described by a known function $g_k(t) = G_k(\mathbf{x}_k(t), \mathbf{x}_{k+1}(t)), t \in [0, T]$ ahead of time based on the trajectory information $\mathbf{x}_k(t)$ and $\mathbf{x}_{k+1}(t)$. For example, such a requirement can be achieved using radio maps, which are data-driven models that map the transmitter and receiver locations to large-scale channel information including path loss and shadowing [12], [13], [14]. Alternatively, one may calculate the channel gain $g_k(t)$ as a function of the distance, such as $g_k(t) = \beta_0 \frac{(d_k(t))^{-\alpha}}{N_0 B}$ [15], [17], [22], where $d_k(t) = \|\mathbf{x}_{k+1}(t) - \mathbf{x}_k(t)\|_2$ is the distance between the kth node and the $(k+1)$th node, β_0 is a channel gain parameter, α is the path loss exponent, N_0 is the noise density, and B is the transmission bandwidth, whereas, the component ξ can be modeled using Rician or Nakagami distribution with parameters chosen based on the LOS condition obtained from a city map.

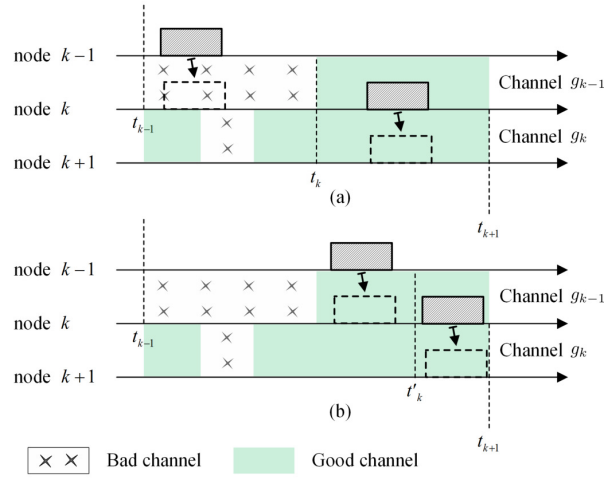

Fig. 2. Cache-and-pass for opportunistic transmission. The challenge is to coordinate the transmission handover time t_k among aerial nodes. (a) A bad coordination results in low energy efficiency due to node $k-1$ transmitting at poor channel conditions. (b) A desired handover time t'_k allows both transmissions to access the good channel.

B. A Hierarchical Formulation for a Mixed Timescale Control

To tackle the challenge from the hierarchical information structure and the requirement of distributed coordination over ad hoc networks, we adopt a *cache-and-pass* transmission framework, where the source data is relayed sequentially from one aerial node to another, and the transmission occurs preferably when the two aerial nodes are closed. In this strategy, as illustrated in Fig. 2, only one link is activated at a time, and hence, there is no UAV-UAV interference.

Correspondingly, we define the *handover time* variable t_k with $0 \le t_1 \le \cdots \le t_K \le T$ for the message passing and local coordination among nodes, where node k only transmits to node $k+1$ in the kth transmission period $[t_k, t_{k+1})$. For notation convenience, we set $t_0 = 0$ and $t_{K+1} = T$. In addition, each node k also has local variables $a_k(t)$ and $p_k(t)$ based on the local information at each node k, where $a_k(t)$ is a 0-1 variable depending on the large-scale channel information $g_k(t)$ to control whether to transmit, and $p_k(t)$ is the power allocation depending on the small-scale channel realization $\hat{g}_k(t)$.

Let ϕ_k be the local policy for node k that maps the channel $g_k(t)$ and $\hat{g}_k(t)$ to the transmission action $a_k(t)$ and the power allocation $p_k(t)$. A policy ϕ_k is eligible if the total expected throughput satisfies the transmission requirement, as

$$\mathbb{E}\left\{\hat{\Upsilon}_k(\phi_k)\right\} \triangleq \int_{t_k}^{t_{k+1}} \mathbb{E}\left\{\hat{c}_k(t)\right\} a_k(t)\, dt \ge S \tag{2}$$

Authorized licensed use limited to: The Chinese University of Hong Kong CUHK(Shenzhen). Downloaded on January 18,2025 at 13:27:52 UTC from IEEE Xplore. Restrictions apply.

where $\hat{c}_k(t) = B\log_2(1 + p_k(t)\hat{g}_k(t))$ is the instantaneous channel capacity, and the expectation is taken over the distribution of the small-scale fading ξ.

Under the policy ϕ_k, the cost of node k is modeled as

$$\hat{E}_k(\phi_k) \triangleq \int_{t_k}^{t_{k+1}} p_k(t)\, a_k(t)\, dt + \lambda \int_{t_k}^{t_{k+1}} a_k(t)\, dt \quad (3)$$

where the first term captures the transmission energy, the second term captures the transmission time, and λ is the weighting factor for the two terms. As pointed out before, minimizing the transmission time, the second term in (3), not only helps reduce the circuit power of the transmitting node, but also reduces the impact of the potential interference leakage from the aerial node.

The goal is to find the handover time t_k and the local policy ϕ_k, such that the total expected cost is minimized[1]

$$\mathscr{P}0: \underset{\{t_k,\phi_k\}}{\text{minimize}} \quad \sum_{k=0}^{K} \mathbb{E}\left\{\hat{E}_k(\phi_k)\right\} \quad (4)$$

$$\text{subject to} \quad \mathbb{E}\left\{\hat{\Upsilon}_k(\phi_k)\right\} \geq S,\ \forall k \quad (5)$$

$$0 \leq t_1 \leq t_2 \leq \cdots \leq t_K \leq T. \quad (6)$$

According to the information structure and the timescales of the control variables, the original problem $\mathscr{P}0$ is reformulated into the following two-layer mixed timescale optimization problems.

1) Inner Layer: A local transmission policy $\phi_k = \{p_k, a_k\}$ is optimized based on the local information $\hat{g}_k(t)$ and $g_k(t)$ by solving the following mixed timescale problem

$$E_k^*(t_k, t_{k+1}) \triangleq \underset{\{p_k(t), a_k(t)\}}{\text{minimize}} \quad \mathbb{E}\left\{\hat{E}_k(\phi_k)\right\} \quad (7)$$

$$\text{subject to } \mathbb{E}\left\{\hat{\Upsilon}_k(\phi_k)\right\} \geq S. \quad (8)$$

Recall that the power allocation $p_k(t)$ is determined at a small timescale for each channel realization $\hat{g}_k(t)$ given $a_k(t)$, whereas the transmission control $a_k(t)$ is determined at a large timescale based on the large-scale channel $g_k(t)$ acquired from the predetermined trajectory of the nodes.

2) Outer Layer: The handover times t_k's are optimized via local coordination based on the following problem

$$\mathscr{P}1: \underset{\{t_k\}}{\text{minimize}} \quad \sum_{k=0}^{K} E_k^*(t_k, t_{k+1}) \quad (9)$$

$$\text{subject to } 0 \leq t_1 \leq t_2 \leq \cdots \leq t_K \leq T \quad (10)$$

where each node k determines t_k based on t_{k-1} and t_{k+1} passed from the neighbors.

III. Inner Layer for the Mixed Timescale Optimization

W.l.o.g., we focus on the transmission on the first link, *i.e.*, the transmission from node $k = 0$ to node 1 in the transmission period $[0, t_1)$. Thus, in this section, we drop the subscript k for notation brevity if the meaning is clear from the context. The problem formulation and algorithm developed for node $k = 0$ naturally apply to other nodes $k = 1, 2, \ldots, K$.

This section aims at developing the mixed timescale transmission strategy ϕ for the power allocation $p(t)$ and transmission indicator $a(t)$ in a transmission period $\mathcal{I} = [0, t_1)$, such that S bits can be transmitted,

A. Small Timescale Optimization for the Power Allocation

It can be easily verified that the optimal power allocation $p(t)$ from the small timescale when given the on-off control $a(t)$ is given by a water-filling solution as follows.

Lemma 1 (Small Timescale Power Allocation): Given any $a(t)$, the optimal power allocation policy takes the form

$$p(t; v) = [v - 1/(\hat{g}(t))]^+ \quad (11)$$

where v is a parameter and $[x]^+$ is defined as $[x]^+ = \max(x, 0)$.

Proof: Given any $a(t)$, the inner problem (7) within the active duration $\{t \in \mathcal{I} : a(t) = 1\}$ becomes a classical convex power allocation problem. Thus, the optimal power allocation strategy must follow $[v - 1/(\hat{g}(t))]^+$, where the optimal choice of v is to satisfy (8) with equality imposed [36]. □

The challenge of implementing solution (11) is the computation of the Lagarangian parameter v^*, which involves iterative computations, and, at each iteration, evaluating a double integral for the expectation and throughput in (8). To circumvent this issue, consider a proxy channel capacity function $c(t) = B\log_2(1 + \kappa p(t) g(t))$, which only depends on the large-scale channel $g(t)$, where κ is a parameter to back-off for the power penalty due to the small-scale fading ξ; and the power allocation $p(t)$ is chosen based on the water-filling solution structure (11) but it only depends on the proxy channel $\kappa g(t)$, specifically, $p(t; v, \kappa) = [v - 1/(\kappa g(t))]^+$. As a result, the proxy channel capacity function is derived as

$$c(t) = B\log_2(\kappa v g(t))\, \mathbb{I}\{\kappa v g(t) > 1\} \quad (12)$$

and a proxy throughput constraint is formulated as

$$\tilde{\Upsilon}(\phi) \triangleq \int_0^{t_1} c(t)\, a(t)\, dt = S. \quad (13)$$

It turns out that, with a proper choice of κ, $c(t)$ can yield a tight lower bound of $\mathbb{E}\{\hat{c}(t)\}$ defined using (2) and (9). This is shown in the following lemma.

Lemma 2: For any v, $\mathbb{E}\{\hat{c}(t)\} \geq c(t)$ for all active time $t \in \mathcal{I}_A = \{t \in \mathcal{I} : a(t) = 1\}$, if and only if

$$\log_2(\kappa) \leq J(\beta) + \mathbb{E}\{\log_2(\xi)\} \quad (14)$$

where $J(\beta) \triangleq \int_0^{\beta} \log_2(\beta/x)\, dF_\xi(x)$, $\beta = (v \sup_{t \in \mathcal{I}_A}\{g(t)\})^{-1}$, and $F_\xi(x) \triangleq \mathbb{P}\{\xi \leq x\}$.

Proof: See Appendix A. □

From (12) and (14), it is clear that a larger κ leads to a tighter lower bound $\mathbb{E}\{\hat{c}(t)\} \geq c(t)$. Therefore, we are interested in the largest value $\bar{\kappa}$ that achieves the equality of (14). Lemma 2 implies that the optimal κ, or equivalently, the optimal v can be found from the following corollary.

[1]Note that one can also maximize the expected throughput $\mathbb{E}\{\hat{\Upsilon}_k(\phi_k)\}$ subject to a constraint related to the expected cost $\mathbb{E}\{\hat{E}_k(\phi_k)\}$. This leads to a dual problem of $\mathscr{P}0$, and a similar approach may apply.

Authorized licensed use limited to: The Chinese University of Hong Kong CUHK(Shenzhen). Downloaded on January 18,2025 at 13:27:52 UTC from IEEE Xplore. Restrictions apply.

Corollary 1: Given $\mu = \kappa v$, the optimal v that minimizes the energy consumption (7) with $\mathbb{E}\{\hat{c}(t)\} \geq c(t)$ is given by the solution to the following equation

$$f_v \triangleq \log_2(\mu/v) - J(\beta) - \mathbb{E}\{\log_2(\xi)\} = 0 \tag{15}$$

where function f_v is monotonically decreasing over v.

Proof: The optimal transmission power $p(t;v)$ defined in (11) is monotonically increasing over v, thus the minimum v leads to the minimal energy consumption in (7) for given $a(t)$. For keeping $\mathbb{E}\{\hat{c}(t)\} \geq c(t)$, inequation (14) must satisfy according to Lemma 2. Substitute $\mu = \kappa v$ in to (14), we have $f_v \leq 0$, where function f_v is monotonically decreasing over v because $df_v/dv = -\mathbb{P}_\xi(x > \beta)/(v \ln 2) < 0$. Thus, the optimal v is the solution to the equation $f_v = 0$. □

Based on Corollary 1, one can find the best parameters κ and v, through a bisection search algorithm due to the monotonicity of f_v.

B. Large Timescale Optimization for a(t) and μ

Corollary 1 suggests that given a feasible parameter μ, one can decouple the optimization for the strategies $p(t)$ and $a(t)$. Consider a proxy policy $\phi = \{p(t), a(t)\}$ with proxy power allocation $p(t) = [v - 1/(\kappa g(t))]^+$, where v and κ are obtained from Corollary 1. A large timescale proxy problem for the on-off control $a(t)$ can be formulated as

$$\underset{a(t)}{\text{minimize}}\ \tilde{E}(\phi), \text{ subject to } \tilde{\Upsilon}(\phi) \geq S \tag{16}$$

where the proxy energy consumption is formulated by

$$\tilde{E}(\phi) \triangleq \int_0^{t_1} [v - 1/(\kappa g(t))]^+ a(t)\, dt + \lambda \int_0^{t_1} a_k(t)\, dt.$$

We will show that a threshold policy for $a(t)$ suffices to achieve the optimality of (16).

For mathematical completeness, we define the notion of *almost identical policy* as follows. Let $m(\mathcal{A})$ be the Lebesgue measure of a set $\mathcal{A}$ on $\mathbb{R}$. For example, $m((a,b)) = b - a$ gives the length of the open interval (a,b) and $m(\mathcal{C}) = 0$ for a countable set $\mathcal{C}$.

Definition 1 (Almost Identical Policy): Consider two transmission indicators $a^{(1)}(t)$ and $a^{(2)}(t)$ defined over the same transmission period $\mathcal{I}$. If $m\left(\left\{t \in \mathcal{I} : a^{(1)}(t) \neq a^{(2)}(t)\right\}\right) = 0$, then the two policies are said to be *almost identical*.

According to the above definition, two policies that differ in a set of time intervals with measure 0 will be considered as almost identical, abbreviated to *identical*, or *the same* thereafter. In practice, the policy difference shorter than a symbol-level duration will not affect the implementation.

1) Strategy Under Continuously Time-Varying Channel: We first consider that the channel $g(t)$ is continuously time-varying. Specifically, let $\zeta(\eta) = m(\{t \in \mathcal{I} : g(t) = \eta\})$ be the *sojourn time* when the channel gain $g(t)$ equals to η. In our context, a continuously time-varying channel means the sojourn time $\zeta(\eta)$ equals to zero for every channel quality η. Such a condition corresponds to the scenario where the distance between the two aerial nodes varies, for example, the two aerial nodes travel in different speeds.

Consider the following *strict threshold policy*

$$a(t;\eta) = \mathbb{I}\{g(t) \geq \eta\} \tag{17}$$

where $\mathbb{I}\{\mathcal{A}\}$ is an indicator function with $\mathbb{I}\{\mathcal{A}\} = 1$, if condition $\mathcal{A}$ is satisfied, and $\mathbb{I}\{\mathcal{A}\} = 0$, otherwise.

It is not surprising to find out that a strict threshold policy is necessary for minimum cost under the continuously time-varying channel.

Lemma 3 (Necessary Condition for Optimality): The optimal transmission indicator function $a(t)$ to solve (16) is identical to a threshold policy $\mathbb{I}\{g(t) \geq \eta\}$.

Proof: See Appendix B. □

As a consequence of Lemma 3, one need not worry about optimizing the transmission indicator $a(t)$ at every t. Instead, under continuously time-varying channel, one only needs to optimize a scalar η to determine the optimal transmission indicator $a(t)$.

However, Lemma 3 is not suitable for the scenario where the channel quality remains constant with non-negligible time. For example, when the channel quality function is $g(t) = 1, \forall t \in [0, t_1)$, we find that the optimal transmission interval is $[0, \exp(1)]$, under $t_1 > \exp(1)$, $S = 1$ bits, $B = \ln 2$ Hz, $\beta_0 = 0$ dB, $\kappa = 0$ dB, and $\lambda = 1$. However, the strict threshold policy $a(t;\eta)$ defined in (17) chooses whether all time when $\eta \leq 1$ or null when $\eta > 1$, which is unable to describe the optimal transmission action. Thus, a generalized policy is needed.

2) Generalized Strategy for Channel With Non-Negligible Sojourn Time: When the channel $g(t)$ has non-negligible sojourn time $\zeta(\eta) > 0$ for some η, there is a set of time intervals with measure greater than zero at $g(t) = \eta$. Such a scenario occurs when the nodes travel at relatively zero speed, e.g., they fly along parallel trajectories, or the predicted channel qualities are quantized into the same level for a certain period. In such a case, the strict threshold policy is not optimal.

In this case, we study a *generalized threshold policy* with two parameters η and τ as follows:

$$a(t;\eta,\tau) = \mathbb{I}\{g(t) > \eta\} + \mathbb{I}\{g(t) = \eta\} \cdot \mathbb{I}\{t \geq \tau\}. \tag{18}$$

The policy allows the nodes to access the channel for a portion of time when the channel remains at a state $g(t) = \eta$. Note that the generalized threshold policy (18) degenerates to a strict threshold policy (17) when the channel sojourn time $\zeta(\eta)$ equals to zero at state η.

The following lemma shows that a generalized threshold policy is sufficient to achieve the minimum cost E^* in (16).

Lemma 4 (Equivalence to a Generalized Threshold Policy): A generalized threshold policy from (18) achieves the minimum objective value in (16).

Proof: See Appendix C. □

Lemma 4 implies that a generalized threshold policy (18) for $a(t)$ suffices to achieve the minimum cost under a general channel $g(t)$. Therefore, instead of optimizing $a(t)$ point-wisely for each time instance t, one only needs to optimize two threshold parameters η and τ.

While the optimization problem for η and τ is still likely non-convex due to the fact that $g(t)$ can take an arbitrary form, it can be shown that the optimal solution η^* is unique.

Authorized licensed use limited to: The Chinese University of Hong Kong CUHK(Shenzhen). Downloaded on January 18,2025 at 13:27:52 UTC from IEEE Xplore. Restrictions apply.

Algorithm 1 Transmission Timing Optimization

Bisection search to determine η^*

1) Set $\tau = t_1$, $\eta_{\min} = \inf\{g(t) : t \in [0, t_1)\}$, $\eta_{\max} = \sup\{g(t) : t \in [0, t_1)\}$;
2) Set $\eta = (\eta_{\max} + \eta_{\min})/2$, if $\tilde{\Upsilon}(\phi) > S$, set $\eta_{\min} = \eta$; otherwise set $\eta_{\max} = \eta$;
3) Repeat step 2) until $|\eta_{\max} - \eta_{\min}|$ is small enough;
4) Set $\eta^* = \eta_{\max}$;

Bisection search to determine τ^* if $\zeta(\eta^*) > 0$

5) Initialize $\eta = \eta^*$, $\tau_{\min} = 0$, $\tau_{\max} = t_1$;
6) Set $\tau = (\tau_{\max} + \tau_{\min})/2$, if $\tilde{\Upsilon}(\phi) > S$, set $\tau_{\min} = \tau$; otherwise set $\tau_{\max} = \tau$;
7) Repeat step 6) until $|\tau_{\max} - \tau_{\min}|$ is small enough;
8) Set $\tau^* = \tau_{\max}$.

Set $\tau^* = t_1$ if $\zeta(\eta^*) = 0$

Proposition 1 (Uniqueness): The optimal solution (η^*, τ^*) for determining $a(t; \eta, \tau)$ in (18) satisfies $\tilde{\Upsilon}(\phi) = S$. In addition, if $g(t)$ is continuous, then η^* is unique.

Proof: See Appendix D. □

It is not difficult to see that there may be multiple solutions for τ^*. Yet, when the channel sojourn time at η^* is zero, it is irrelevant to specify the threshold τ, because in the second term in (18), $\mathbb{I}\{g(t) = \eta^*\} = 0$ almost everywhere along t.

When the channel sojourn time at η^* is *non-zero*, we will show that there exists a bisection-type algorithm that converges to a globally optimal solution τ^*. This is due to the monotonicity of function $\tilde{\Upsilon}(\phi)$ over η and τ. Specifically, consider two proxy policies $\phi_1 = \{p(t), a_1(t)\}$ and $\phi_2 = \{p(t), a_2(t)\}$, where $a_1(t)$ and $a_2(t)$ are defined in (18). We have the following result.

Proposition 2 (Monotonicity): For any $\eta_1 > \eta_2$ and $\tau_1, \tau_2 \in [0, t_1)$, it holds that $\tilde{\Upsilon}(\phi_1) \leq \tilde{\Upsilon}(\phi_2)$. For any $\tau_1 > \tau_2$ and $\eta \geq 0$, it holds that $\tilde{\Upsilon}(\phi_1) \leq \tilde{\Upsilon}(\phi_2)$.

Proof: See Appendix D. □

Based on the monotonicity, the optimal thresholds η^* and τ^* can be found using bisection search as described in Algorithm 1, which is shown to converge.

Proposition 3 (Convergence): Algorithm 1 converges, and the converged values η^* and τ^* is the optimal solution.

Proof: See Appendix E. □

3) The Overall Algorithm: The large timescale parameters κ, v, η, and τ for the power allocation policy $p(t)$ and the on-off control policy $a(t)$ can be determined by

$$\begin{aligned} \underset{\mu \geq 0}{\text{minimize}}\ & E^*(\mu) \triangleq \min_{\kappa, v, \eta, \tau} \tilde{E}(\phi) \\ \text{s.t.}\ & \log_2 \kappa \leq J(\beta) + \mathbb{E}\{\log_2(\xi)\} \\ & \tilde{\Upsilon}(\phi) \geq S. \end{aligned}$$

Based on the previous discussion, the parameters κ and v can be efficiently found by Corollary 1 and η and τ can be found by Algorithm 1.

Minimizing $E^*(\mu)$ requires a one-dimension scalar search for $\mu > 0$. It turns out from our numerical study that $E^*(\mu)$ appears as a bowl-shaped quasi-convex function. Fig. 3(a) shows different forms of ordered channels $\tilde{g}(t)$. Specifically,

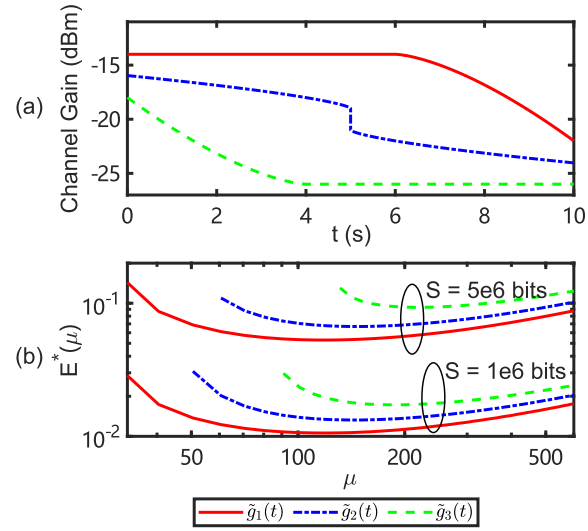

Fig. 3. (a) Three channel gain examples. (b) $E^*(\mu)$ under different channel gain examples and data sizes S. It is observed that $E^*(\mu)$ in terms of μ is a bowl-shaped function.

the ordered channel function $\tilde{g}(t)$ is constructed by permuting the time index t of $g(t)$, such that $\tilde{g}(t) = g(\sigma(t))$ is non-increasing, where $\sigma(t)$ is a permutation function.[2] It is observed from Fig. 3 (b) that, in all the cases, $E^*(\mu)$ first decreases then increases even when $\tilde{g}(t)$ is discontinuous or non-smooth. As a result, the solution μ^* can be easily found using a bisection-type search.

The intuition that $E^*(\mu)$ is likely a bowl-shaped function is that, first, a small μ, corresponding to low signal-to-noise ratio (SNR), may require a long transmission duration, where a portion of data has to be transmitted under relatively poor channel quality, resulting in low power efficiency and high total cost. On the other hand, a large μ, corresponding high SNR, may concentrate the transmission at the high channel quality moment due to the threshold policy (18); however, it is known that it is energy-inefficient for data transmission at high SNR due to the strict concavity of the logarithm function, and therefore, the total cost will also be high.

The computational complexity of inner-layer strategy is $\mathcal{O}(T\log(T)\log^2(\varepsilon^{-1}))$, where ε is the required solution precision. This consists of $\mathcal{O}(\log(\varepsilon^{-1}))$ steps for one-dimension scalar search of μ^*, and $\mathcal{O}(T\log(T\varepsilon^{-1}))$ steps for bisection search of η^* and τ^*, where it needs $\log(T\varepsilon^{-1})$ times of $\mathcal{O}(T)$ for calculating $\tilde{\Upsilon}(\phi)$.

IV. Outer Layer for the Large Timescale Team Decision Problem

This section aims at developing a team strategy to solve problem $\mathscr{P}1$ for the handover time t_k's. As it is formulated in Section II, the set of nodes aims at minimizing the total cost in (9), where each node k only has the local information on the large timescale channel gain $g_k(t)$ and $g_{k-1}(t)$, *i.e.*, the

[2]It is clear that under the generalized threshold policy, two channels $g(t)$ and $g'(t)$ result in the same energy function $\tilde{E}(\phi)$ as long as both $g(t)$ and $g'(t)$ map to the same ordered channel function $\tilde{g}(t)$. As a result, the ordered channel function $\tilde{g}(t)$ can represent a large amount of channel functions $g(t)$ by permuting the time index.

Authorized licensed use limited to: The Chinese University of Hong Kong CUHK(Shenzhen). Downloaded on January 18,2025 at 13:27:52 UTC from IEEE Xplore. Restrictions apply.

channels connected to the neighbors of node k. As a result, each node k only has access to the local cost

$$\Lambda_k\left(t_k, \boldsymbol{t}_{-k}\right) = E_{k-1}^*\left(t_{k-1}, t_k\right) + E_k^*\left(t_k, t_{k+1}\right) \tag{19}$$

which contributes to a portion of the global cost in (9). Here, the variable $\boldsymbol{t}_{-k} \triangleq \{t_j\}_{j \neq k}$ is a collection of handover time to be determined by nodes other than k. Recall that $E_k^*\left(t_k, t_{k+1}\right)$ is the minimum cost that is achieved under the optimal mixed timescale transmission strategy over $p_k(t)$ and $a_k(t)$ computed in Section III, given the transmission period t_k and t_{k+1}.

A. Solution via a Game Reformulation

The distributed structure of the cost and information naturally leads to a game for the handover time

$$\begin{aligned} \mathcal{G}: \underset{t_k}{\text{minimize}} \quad & \Lambda_k\left(t_k, \boldsymbol{t}_{-k}\right) \\ \text{subject to } & t_{k-1} \leq t_k \leq t_{k+1} \end{aligned}$$

for all $k \in \mathcal{K}$, where $\mathcal{K} = \{1, 2, \cdots, K\}$ is the set of nodes (players of the game). Denote $\boldsymbol{\mathcal{T}}$ as the set of possible combinations of the transmission space, $\mathcal{T}_k = [t_{k-1}, t_{k+1}]$ as the strategy space of node k, and $\boldsymbol{\mathcal{T}}_{-k}$ as the set of possible combinations of the transmission space of all nodes except for node k, such that the constraint $0 \leq t_1 \leq t_2 \leq \cdots \leq t_K \leq T$ holds.

The notation of NE of $\mathcal{G}$ is defined as follows. A set of handover time $\boldsymbol{t}^* = (t_1^*, t_2^*, \cdots, t_K^*)$ is called an NE (in pure strategies) if and only if (iff) the following holds: $\Lambda_k\left(t_k^*, \boldsymbol{t}_{-k}^*\right) \leq \Lambda_k\left(t_k, \boldsymbol{t}_{-k}^*\right), \forall t_k \in \mathcal{T}_k, \forall k \in \mathcal{K}$. The NE in the handover time game is a handover time allocation profile $\{t_k\}$ for all the nodes in the network that none of the nodes can benefit from changing its own handover time unilaterally. The notion of the NE thus characterizes the situation where the nodes reach an agreement on the handover time allocation.

To study the existence and property of the NE, we exploit the notion of *potential game* defined as follows.

Definition 2 (Exact Potential Game): A game is called an exact potential game, if there exists a function $\psi : \boldsymbol{\mathcal{T}} \to \mathbb{R}$ such that for all $k = 1, 2, \cdots, K$, for all $\boldsymbol{t}_{-k} \in \boldsymbol{\mathcal{T}}_{-k}$, and for all $t_k', \ t_k'' \in \mathcal{T}_k$, the following equation holds:

$$\psi\left(t_k', \boldsymbol{t}_{-k}\right) - \psi\left(t_k'', \boldsymbol{t}_{-k}\right) = \Lambda_k\left(t_k', \boldsymbol{t}_{-k}\right) - \Lambda_k\left(t_k'', \boldsymbol{t}_{-k}\right).$$

Moreover, the function ψ is called a potential function.

Based on Definition 2, in an exact potential game, the change in the utility of a node due to its own strategy deviation results in exactly the same amount of change in the potential function.

It turns out that the handover time game $\mathcal{G}$ is an exact potential game.

Proposition 4: Game $\mathcal{G}$ is an exact potential game with a potential function given by $\psi(\boldsymbol{t}) = \sum_{k=0}^{K} E_k^*\left(t_k, t_{k+1}\right)$. In addition, there exists an NE in game $\mathcal{G}$.

Proof: See Appendix F. □

Note that the potential function is exactly the objective function of $\mathscr{P}1$. Using the property of a potential game, we establish the relationship between the NEs of $\mathcal{G}$ and the solution to $\mathscr{P}1$.

Proposition 5 (Connection Between the NE and the Solution to $\mathscr{P}1$): i) If $\boldsymbol{t}^*$ is an optimal solution to $\mathscr{P}1$, then $\boldsymbol{t}^*$ is an NE of $\mathcal{G}$; ii) Suppose that the functions Λ_k are differentiable. If $\boldsymbol{t}^*$ is an NE of $\mathcal{G}$, then $\boldsymbol{t}^*$ is a stationary point of $\mathscr{P}1$.

Proof: See Appendix G. □

Therefore, we solve problem $\mathscr{P}1$ by searching for the NE of $\mathcal{G}$. In an ideal case where the potential function has a unique stationary point, searching for the NE is equivalent to solving problem $\mathscr{P}1$.

B. Neighbor Coordinate Response

Here, we derive a distributed strategy to reach an NE. Assume that each node k updates its strategy t_k via a *better response*

$$\pi_k(\boldsymbol{t}) = \left\{t_k^\star \in \mathcal{T}_k : \Lambda_k\left(t_k^\star, \boldsymbol{t}_{-k}\right) < \Lambda_k\left(t_k, \boldsymbol{t}_{-k}\right)\right\}; \tag{20}$$

or the *best response*

$$\pi_k(\boldsymbol{t}) = \left\{t_k^\star \in \mathcal{T}_k : t_k^\star = \arg\min_{t_k \in \mathcal{T}_k} \Lambda_k\left(t_k, \boldsymbol{t}_{-k}\right)\right\} \tag{21}$$

based on the updated strategy from its neighbors.

However, under a distributed mechanism, the game is not guaranteed to converge. For example, it may happen that two nodes simultaneously update their strategies, and it takes time for their updated strategies to propagate to all the other nodes in the game. It is known that such a scenario may lead to oscillation between two solutions [37]. On the other hand, sequential update is known to converge to an NE of a potential game [38, Theorem 2.7], and it can be implemented in a distributive way using token passing from one node to another. However, sequential update is highly inefficient as the number of nodes grows. Therefore, the challenge here is to design a distributed mechanism that is guaranteed to converge to an NE and is more efficient than a sequential update.

With such a goal, we develop a distributed strategy based on the notion of *independent group*.

Definition 3: (Dependent Node and Independent Group): Node k depends on node j if the strategy t_j of node j affects the response $\pi_k(\boldsymbol{t})$ of node k. An independent group under game $\mathcal{G}$ is a set of nodes that none of them depends on the strategies of the others.

Note that, in game $\mathcal{G}$, the set of odd-number nodes forms an independent group, and the set of even-number nodes forms another independent group. This is because the only strategies that can affect the response $\pi_k(\boldsymbol{t})$ of any node k are t_{k-1} and t_{k+1}, which are controlled by the counter-parity nodes. Based on the property of independent groups, we propose the following *neighbor coordinate* strategy:

- Each update is associated with a token n, indicating the nth update from node k, and the tuple $\left(t_k^{(n)}, n\right)$ is passed to the neighbors when the nth update is computed.
- For each odd-number node, compute the $(n+1)$th round response by solving Equations (20) or (21) based on the nth response $\left(t_k^{(n)}, n\right)$ from its neighbors.
- For each even-number node, compute the $(n+1)$th round response by solving Equations (20) or (21) based on the $(n+1)$th response $\left(t_k^{(n+1)}, n+1\right)$ from its neighbors.

Authorized licensed use limited to: The Chinese University of Hong Kong CUHK(Shenzhen). Downloaded on January 18,2025 at 13:27:52 UTC from IEEE Xplore. Restrictions apply.

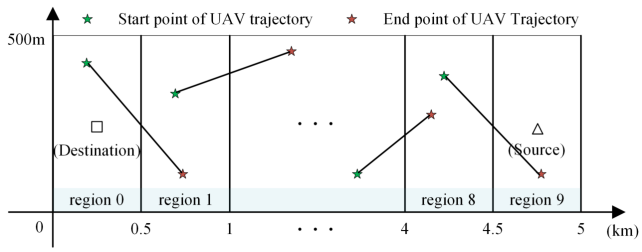

Fig. 4. Illustration of aerial ad hoc network assisted data collection scenarios generating.

The proposed update strategy is more efficient than a conventional sequential update because half of the nodes are allowed to compute their updates in parallel. In addition, it also avoids the potential convergence issue from parallel update, because the token passing mechanism guarantees that if the strategies of two nodes depend on each other, the two nodes are not allowed to update simultaneously. We formally establish the convergence results as follows.

Proposition 6 (Convergence): The neighbor coordinate update with better or best response converges to an NE of game $\mathcal{G}$.

Proof: See Appendix H. □

There are two major sources of signaling overhead: trajectory information exchange and coordination. For the coordination, each node updates its own handover time t_k based on the neighbors' decisions t_{k-1} and t_{k+1}, and passes the updated t_k to the two neighbors. As a result, each node only needs to communicate 3 scalars with the neighbors for each iteration. On the other hand, the trajectory information is only exchanged with the neighbors before the coordination. As the trajectory is usually piecewise linear for cargo delivery and many patrol surveillance acpluav, the overall signaling overhead is small.

The overall computational complexity is $\mathcal{O}(T\log^2(T)\log^3(\varepsilon^{-1}))$ or simply $\mathcal{O}(T\log^2(T))$, which consists of $\mathcal{O}(\log(T\varepsilon^{-1}))$ steps (for better response) of $\mathcal{O}(T\log(T\varepsilon^{-1}))$ for calculating $E_k^*(t_k, t_{k+1})$.

V. Numerical Results

Consider a 5 km × 500 m area partitioned into 10 regions and aerial nodes deployed in the area as shown in Fig. 4. The trajectories of the aerial nodes are generated randomly such that each aerial node travels between two adjacent regions. The aerial nodes may suspend the communication service at the end points with a random duration following a uniform distribution $\mathcal{U}(0, D)$. The destination is at a fixed location in the center of the first region. The source locates uniformly at random in region 1 to 9. For a source located in region K, a team of K aerial nodes each traveling over one of the regions from 1 to K are chosen for data transportation as discussed in Section II.

In this section, numerical results are provided to validate the proposed design. The source, destination, and aerial node altitudes are fixed at 0 m, 50 m, and 120 m. The aerial node velocity is set randomly at 30-50 m/s [15], [39] to simulate transporting data from a sensor to a fusion center.

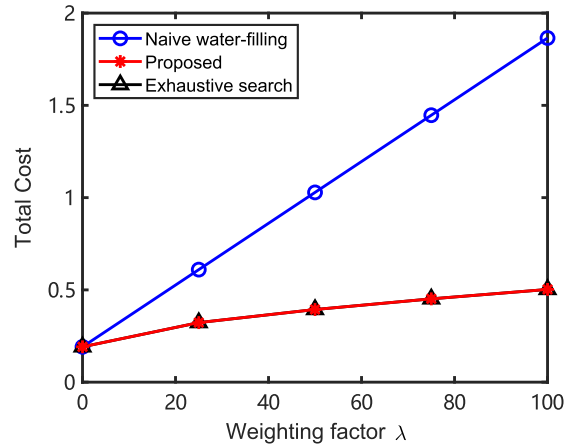

Fig. 5. Cost over different small timescale transmission strategies under different weighting factors.

The communication bandwidth is $B = 10$ MHz and the noise power spectrum density is $N_0 = -169$ dBm/Hz. We simulate the channel gain as $g_k(t) = \xi\beta_0(N_0B)^{-1}d_k^{-\alpha}(t)$, where $\beta_0 = -60$ dB and ξ is a stationary random process following an exponential distribution with mean 1 to model the small-scale fading. Note that the realization ξ is unknown to the system.

A. Performance of the Mixed Timescale Transmission

We evaluate the following schemes for the comparison with the proposed mixed timescale transmission strategy for power allocation and sleep mode aware transmission timing optimization.

1) Naive Water-Filling: This strategy first solve problem (7) to obtain $p^*(t)$ by forcing $a(t) = 1$, then, construct the transmission policy by $a(t) = \mathbb{I}\{p^*(t) > 0\}$. Note that although such a scheme also allows a sleep mode to save the cost whenever $a(t) = 0$, it is not a joint design with the on-off control.

2) Water-Filling With Exhaustive Search: This strategy utilizes the proposed thresholding proxy policy and finds out the optimal parameter μ^* by exhaustive search.

Fig. 5 illustrates the total cost under different weighting factor settings. It is shown that the proposed strategy based on thresholding proxy policy outperforms the naive water-filling strategy, where the proposed scheme requires substantially low energy when the weighting factor is high. In addition, the proposed scheme achieves almost identical performance to the exhaustive search scheme. This confirms that the proposed thresholding proxy policy is already practically good enough for achieving the global optimality.

B. Performance of the Large Timescale Team Strategy

We evaluate the performance of the following baseline schemes that also exploit the trajectory information, but use different strategies to coordinate the transmission among aerial nodes.

1) Relay Without Caching (Constant Transmission Power): The aerial nodes relay the data from the source to the destination directly via multi-hop transmission without caching.

Authorized licensed use limited to: The Chinese University of Hong Kong CUHK(Shenzhen). Downloaded on January 18,2025 at 13:27:52 UTC from IEEE Xplore. Restrictions apply.

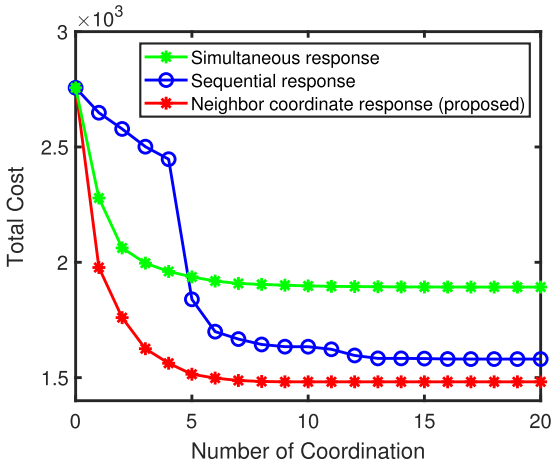

Fig. 6. Performance improvement with the round of response. Faster convergence is observed.

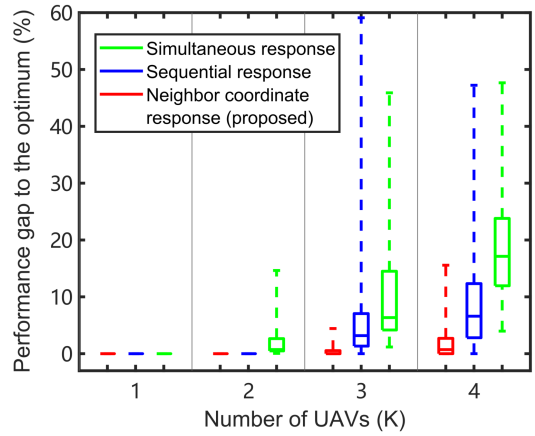

Fig. 7. Performance gap to the optimum over different numbers of UAVs. The lines in the boxplot, from bottom to top, represent the minimum, 25th percentile, median, 75th percentile, and maximum of the sample, respectively.

The aerial nodes transmit the data through the $(K+1)$-hop relay channel using a decode-and-forward strategy with half-duplex mode for each node. The instantaneous capacity is $\frac{1}{K+1}\min_k\{c_k(t)\}$, and the transmission timing $a(t)$ and constant power allocation p is determined in a centralized way based on the effective channel $\bar{g}(t) \triangleq \min_k\{g_k(t)\}$ and the *global* trajectory information, and using the proposed mixed timescale transmission strategy developed in Section III.

2) Relay Without Caching (Optimized Transmission Power) [26]: This strategy optimizes the transmission power $p_k(t)$ for every node over the entire horizon $t \in [0, T]$ using a centralized algorithm based on global information; however, no data caching is used. Specifically, the transmission power is optimized by solving

$$\underset{p_k(t)\geq 0}{\text{minimize}} \quad \frac{1}{K+1}\sum_{k=0}^{K}\int_0^T p_k(t)\,dt$$
$$\text{subject to} \quad \int_0^T \bar{c}(t)\,dt \geq S$$

where $\bar{c}(t) \triangleq \frac{1}{K+1}\min_{k\in\{0,1,\cdots,K\}}\{\log(1+p_k(t)g_k(t))\}$ is the effective capacity for end-to-end transmission.

3) Data Ferry Without Coordination: The cache-and-pass strategy introduced in Section II-B and the proposed power allocation and transmission timing strategy developed in Section III are used, but the handover time is blindly determined as equal interval, $t_k = kT/(K+1)$, $k \in \mathcal{K}$.

Fig. 6 shows the convergence under the number of coordinations, where the better response is used. For numerical stability, the update of simultaneous response is performed as $t_k^{(n+1)} = \vartheta t_k^* + (1-\vartheta)\,t_k^{(n)}$, where t_k^* is the response in $(n+1)$ round, and $\vartheta = 0.25$ is update ratio. It is shown that the proposed neighbor coordination response strategy can converge to an NE with a faster speed, almost reaching NE after 8 rounds of coordination.

Fig. 7 illustrates the performance gap of different response methods compared to the optimum, which is presented by the exhaustive searching algorithm. It is shown that as the number of UAVs increases, the solutions obtained from all three response methods typically become more sub-optimal.

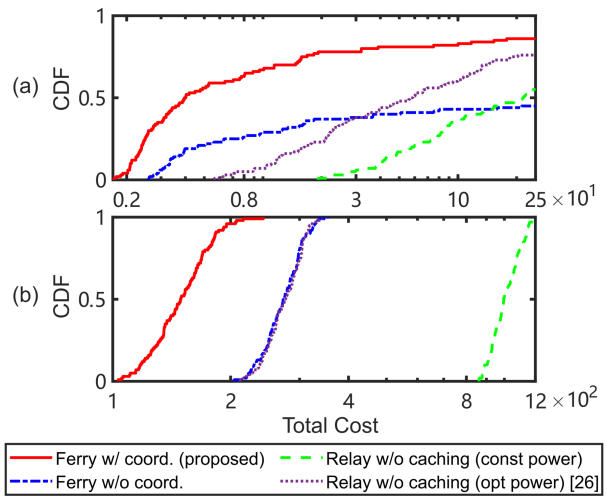

Fig. 8. The cumulative distribution function (CDF) of total cost under different tolerable time T, and communication service suspension time D: (a) $T = 15$ s $D = 5$ s; (b) $T = 5$ s, $D = 0$ s, where data size $S = 100$ Mbits.

This is because all three response methods converge to local optimal points, and the number of these local optimal points increases as the number of UAVs increases. However, the proposed method outperforms the others; our performance gap to the optimum is negligible, less than 0.8% in the median even for $K = 4$, while the ones for sequential response and simultaneous response are 6.5% and 17%, respectively.

Fig. 8 shows the cumulative distribution function (CDF) of total cost under different tolerable times and communication service suspension times, where $K = 5$, $\lambda = 10$, and $\beta = -50$ dB. As shown in Fig. 8, the transmission scheme with smart power control through centralized coordination can approach the performance of the data ferry without a coordination scheme. This verifies that the caching strategy can better use the communication channel; Even without global information, the caching scheme with a trivial handover time policy can perform similarly to the no-caching scheme through centralized coordination. However, it still exhibits an order of performance gap compared to the proposed scheme with handover time coordination.

Authorized licensed use limited to: The Chinese University of Hong Kong CUHK(Shenzhen). Downloaded on January 18,2025 at 13:27:52 UTC from IEEE Xplore. Restrictions apply.

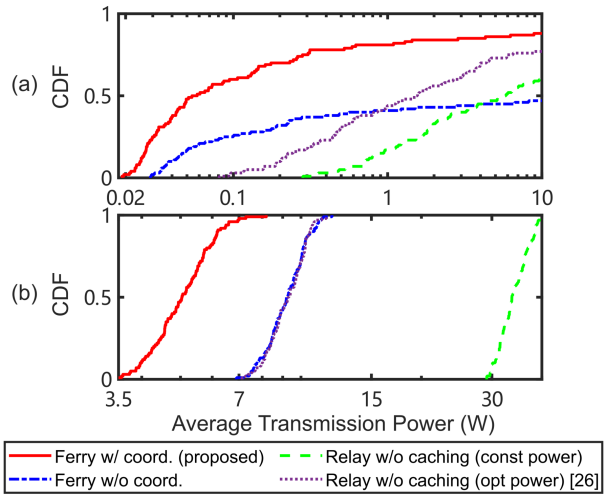

Fig. 9. The CDF of average transmission power (when the transmission is active) under different tolerable time T, and communication service suspension time D: (a) $T = 15$ s $D = 5$ s; (b) $T = 5$ s, $D = 0$ s, where data size $S = 100$ Mbits.

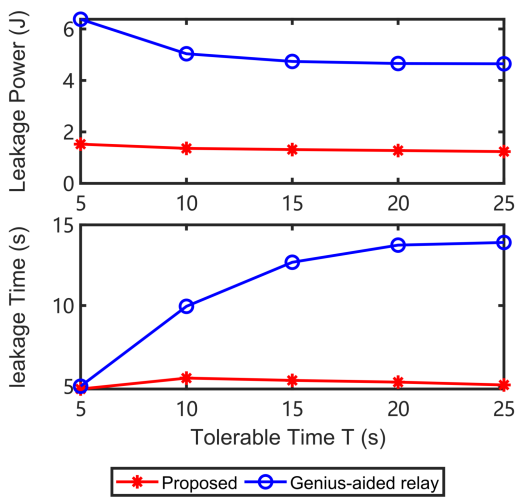

Fig. 10. Comparison of leakage power and time over different tolerable times T, where the data size $S = 10$ Mbits, source location region $K = 5$.

Fig. 9 shows the performance of different schemes on average transmission power (when the transmission is active), which is computed as $(\sum_{k=0}^{K}\int_0^T p_k(t)a_k(t)dt)/(\sum_{k=0}^{K}\int_{t_k}^{t_{k+1}} a_k(t)dt)$. It is observed that the baseline schemes emit more than 10 times more power than the proposed scheme on average. It implies that the proposed scheme can achieve an order-of-magnitude reduction in interference leakage to ground users.

Fig. 10 shows the leakage power and time over different tolerable times, where the baseline, genius-aided relay that is the upper bound of constant power transmission by the immediate reaction, sets the transmission power by exhaustively searching. It is observed that the proposed two-layer delay-tolerant data transportation strategy makes better usage of tolerable time and reduces both leakage power and time. Note that within 25 seconds of tolerable time, the dedicated-deployment UAV is unable to finish the data transmission from the sensor to the fusion center with about 2.5 km because of the flight speed limit.

VI. Conclusion

This paper designed a two-layer delay-tolerant data transportation strategy over dynamic aerial ad hoc networks with trajectory information. In the inner layer, it is theoretically proved that the best power allocation and transmission timing can be constructed using a thresholding proxy policy. Based on this, a transmission power and timing optimization algorithm is developed. In the outer layer, the handover time coordination problem is formulated by a game theoretical approach, and the handover time game is proved to be a potential game, and consequently, the NEs are stationary points of the original problem. Simulation verified that the thresholding proxy policy achieves almost identical performance of the one under exhaustive search. Numerical results showed that the proposed game-based handover time coordination strategy demonstrates substantially better performance guarantee over conventional schemes even though they also exploit the trajectory information. In addition, the proposed distributive mechanism, neighbor coordinate response, is shown to accelerate the convergence to an NE, and achieve almost global optimality.

Appendix A
Proof of Lemma 2

When $v\kappa g(t) \leq 1$, $c(t) = 0$ according to (12), then $\mathbb{E}\{\hat{c}(t)\} \geq c(t)$ because $\mathbb{E}\{\hat{c}(t)\} \geq 0$. When $v\kappa g(t) > 1$, the proxy channel capacity becomes $c(t) = B\log_2(v\kappa g(t))$. Substitute $\hat{g}(t) = g(t)\xi$ according to (1) into the expected channel capacity function, we have

$$\begin{aligned}\mathbb{E}\{\hat{c}(t)\} &= \mathbb{E}\left\{B\log_2\left(1+[v-1/(\hat{g}(t))]^+\hat{g}(t)\right)\right\}\\ &= \mathbb{E}\{B\log_2(v\hat{g}(t))\,\mathbb{I}\{v>1/\hat{g}(t)\}\}\\ &= B\log_2(vg(t))\,\mathbb{P}\left\{\xi>(vg(t))^{-1}\right\}\\ &\quad+\mathbb{E}\left\{B\log_2(\xi)\,\mathbb{I}\left\{\xi>(vg(t))^{-1}\right\}\right\}.\end{aligned}$$

Denote $\beta \triangleq 1/(vg(t))$, we have

$$\begin{aligned}\frac{\mathbb{E}\{\hat{c}(t)\}}{B} &= \log_2\left(\beta^{-1}\right)\mathbb{P}\{\xi>\beta\}+H(\beta)\\ &= \log_2\left(\beta^{-1}\right)(\mathbb{P}\{\xi>\beta\}-1+1)+H(\beta)\\ &= \log_2(\beta)F_\xi(\beta)+\log_2\left(\beta^{-1}\right)+H(\beta)\\ &= \int_0^\beta \log_2(\beta)-\log_2(x)\,dF_\xi(x)\\ &\quad+\int_0^\beta \log_2(x)\,dF_\xi(x)+\log_2\left(\beta^{-1}\right)+H(\beta)\\ &= J(\beta)+\log_2(vg(t))+\mathbb{E}\{\log_2(\xi)\}\\ &= \frac{c(t)}{B}+J(\beta)+\mathbb{E}\{\log_2(\xi)\}-\log_2(\kappa)\end{aligned}\tag{22}$$

where $H(\beta) \triangleq \mathbb{E}\{\log_2(\xi)\mathbb{I}\{\xi>\beta\}\}$, $F_\xi(x) \triangleq \mathbb{P}\{\xi \leq x\}$, and $J(\beta) \triangleq \int_0^\beta \log_2(\beta/x)\,dF_\xi(x)$. Note that $H(0) = \mathbb{E}\{\log_2(\xi)\}$ and function $J(\beta)$ is increasing function over β.

It follows from (22) that $\mathbb{E}\{\hat{c}(t)\} \geq c(t)$ for all active time $t \in \mathcal{I}_A$ if and only if $J(\beta)+\mathbb{E}\{\log_2(\xi)\}-\log_2(\kappa) \geq 0$ for all $\beta = 1/(vg(t))$ and $t \in \mathcal{I}_A$. This leads to the condition (14) and Lemma is thus proven.

Authorized licensed use limited to: The Chinese University of Hong Kong CUHK(Shenzhen). Downloaded on January 18,2025 at 13:27:52 UTC from IEEE Xplore. Restrictions apply.

APPENDIX B
PROOF OF LEMMA 3

Denote the energy efficiency under proxy power allocation of each time t as $e(t) = c(t; v, \kappa)/(p(t; v, \kappa) + \lambda)$, the energy efficiency is increasing over the channel quality $g(t)$ when $p(t; v, \kappa) > 0$, *i.e.*, $\kappa v g(t) \geq 0$. When $\kappa v g(t) \geq 0$, the energy efficiency function is $e(t) = B \log_2(\kappa v g(t))/(v - 1/(\kappa g(t)) + \lambda)$, which is increasing over $g(t)$ because its first derivative over $g(t)$ is

$$\frac{\partial e(t)}{\partial g(t)} = \frac{-B\kappa \left(\ln\left(\kappa v g\left(t\right)\right) - \kappa\left(\lambda + v\right) g\left(t\right) + 1\right)}{\ln 2 \left(\kappa\left(\lambda + v\right) g\left(t\right) - 1\right)^2}$$

where the function $\ln(\kappa v g(t)) - (\lambda + v)\kappa g(t) + 1$ is concave over $g(t)$, and has maximum $\ln(v/(\lambda + v)) < \ln(1) < 0$ on $g(t) = 1/(\kappa\lambda + \kappa v)$ where its first is derivative equal to 0. Thus, $\partial e(t)/\partial g(t)$ is always greater than 0.

Let $a(t)$ be the optimal on-off policy given μ. Define the set

$$\mathcal{I}_A = \{t \in [0, t_1) : a\left(t\right) = 1\} \tag{23}$$

as the active interval when transmission occurs, and $\mathcal{I}_A^c = [0, t_1) \backslash \mathcal{I}_A$ as the inactive interval when there is no transmission. It is obvious that $p(t) > 0$ for $t \in \mathcal{I}_A$, otherwise, it will consume cost λ but have no contribution on throughput.

In order to define the minimum and maximum channel gain during a subset without the influence of singleton points, we define the essential supremum and essential infimum first as follow:

Definition 4 (Essential Supremum and Essential Infimum): Let $f : \mathcal{X} \to \mathbb{R}$ be a measurable real valued function defined on a set $\mathcal{X}$. Essential supremum is the minimum value a, such that the set $\{x \in \mathcal{X} : f\left(x\right) > a\}$ has a measure of 0, that is, $\operatorname{ess\,sup} f = \inf\left\{a \in \mathbb{R}, m\left(\left\{x \in \mathcal{X} : f\left(x\right) > a\right\}\right) = 0\right\}$. Similarly, the essential infimum is defined as $\operatorname{ess\,inf} f = \sup\left\{a \in \mathbb{R}, m\left(\left\{x \in \mathcal{X} : f\left(x\right) < a\right\}\right) = 0\right\}$.

The minimum expected channel gain during the active interval $\mathcal{I}_A$ and the maximum expected channel gain during the inactive interval $\mathcal{I}_A^c$ are respectively denoted as

$$M_1 = \operatorname{ess\,inf}\left\{g\left(t\right) : t \in \mathcal{I}_A\right\} \tag{24}$$

$$M_2 = \operatorname{ess\,sup}\left\{g\left(t\right) : t \in \mathcal{I}_A^c\right\}. \tag{25}$$

According to the following lemma, we have M_1 must be equal or greater than M_2.

Lemma 5: For the optimal policy ϕ, there must be $M_1 \geq M_2$.

Proof: We show that $M_1 \geq M_2$ using contradictions. Suppose that $M_1 < M_2$. Then, define $M_0 = (M_1 + M_2)/2$ and construct intervals $\mathcal{S}_A = \left\{t \in \mathcal{I}_A : M_1 < g\left(t\right) < M_0\right\}$ and $\mathcal{S}'_A = \left\{t \in \mathcal{I}_A^c : M_0 < g\left(t\right) < M_2\right\}$. We have the measure $m(\mathcal{S}_A) > 0$, because otherwise, the minimum channel gain during the active interval would be M_0, which contradicts to (24). Similarly, $m(\mathcal{S}'_A) > 0$. As a result, one can construct two subsets $\mathcal{S}_1 \subset \mathcal{S}_A$ and $\mathcal{S}_2 \subset \mathcal{S}'_A$, such that $\int_{\mathcal{S}_2} p(t) + \lambda dt = \int_{\mathcal{S}_1} p(t) + \lambda dt > 0$, with $|\mathcal{S}_2| < |\mathcal{S}_1|$ because $p(t)$ for $t \in \mathcal{S}_2$ is larger. Based on this, one can construct a new on-off policy $a'(t)$, where $a'(t) = \mathbb{I}\left\{t \in (\mathcal{I}_A \backslash \mathcal{S}_1) \cup \mathcal{S}_2\right\}$.

The following can be observed for policy $a'(t)$: (i) the cost E in problem (16) under $a'(t)$ is the same as for $a(t)$ because the sum of the active cost are equal. (ii) the throughput in problem (16) under $a'(t)$ is greater because the throughput over policy $a'(t)$ is

$$\begin{aligned}
&\int_{\mathcal{I}_A \backslash \mathcal{S}_1} c\left(t\right)\, dt + \int_{\mathcal{S}_2} c\left(t\right) dt \\
&\overset{(a)}{>} \int_{\mathcal{I}_A \backslash \mathcal{S}_1} c\left(t\right)\, dt + \int_{\mathcal{S}_2} c\left(t\right) dt + \underline{e} \int_{\mathcal{S}_2} \lambda dt - \underline{e} \int_{\mathcal{S}_1} \lambda dt \\
&\overset{(b)}{\geq} \int_{\mathcal{I}_A \backslash \mathcal{S}_1} c\left(t\right)\, dt + \int_{\mathcal{S}_2} \underline{e} p\left(t\right) dt + \underline{e} \int_{\mathcal{S}_2} \lambda dt - \underline{e} \int_{\mathcal{S}_1} \lambda dt \\
&\overset{(c)}{=} \int_{\mathcal{I}_A \backslash \mathcal{S}_1} c\left(t\right)\, dt + \underline{e} \int_{\mathcal{S}_1} p\left(t\right) dt \\
&\overset{(d)}{>} \int_{\mathcal{I}_A \backslash \mathcal{S}_1} c\left(t\right)\, dt + \int_{\mathcal{S}_1} \overline{e} p\left(t\right) dt \\
&\overset{(e)}{\geq} \int_{\mathcal{I}_A \backslash \mathcal{S}_1} c\left(t\right)\, dt + \int_{\mathcal{S}_1} c\left(t\right) dt
\end{aligned}$$

where $\underline{e} = \operatorname{ess\,inf}\{e(t) : t \in \mathcal{S}_2\}$ and $\overline{e} = \operatorname{ess\,sup}\{e(t) : t \in \mathcal{S}_1\}$, (a) holds because $|\mathcal{S}_2| < |\mathcal{S}_1|$, (b) and (e) hold because the energy efficiency $e(t)$ is increasing over $g(t)$, (c) holds because $\int_{\mathcal{S}_2} p(t) + \lambda dt = \int_{\mathcal{S}_1} p(t) + \lambda dt$, and (d) holds because $\underline{e} > M_0 > \overline{e}$ due to $\mathcal{S}_1 \subset \mathcal{S}_A$ and $\mathcal{S}_2 \subset \mathcal{S}'_A$. Consequently, one can find a smaller active time $a''(t)$ such that the same throughput S in (16) but requires less energy. This suggests that the on-off policy $a\left(t\right)$ is strictly sub-optimal, contradicting to the hypothesis. As a result, for the optimal on-off policy $a(t)$, there must be $M_1 \geq M_2$. □

Then, under $M_1 \geq M_2$, as shown in the following lemma, policy $a\left(t\right)$ is identical to a threshold policy $a'\left(t\right) = \mathbb{I}\left\{g\left(t\right) \geq M_1\right\}$, which confirms the result in Lemma 3.

Lemma 6: If the channel sojourn time $\zeta\left(M_1\right) = 0$, the optimal policy $a\left(t\right)$ is almost identical to a threshold policy.

Proof: For policy $a\left(t\right)$, partition the active set $\mathcal{I}_A$ in (23) into two parts, $\mathcal{I}_A = \mathcal{I}_{A,1} \cup \mathcal{I}_{A,2}$, where $\mathcal{I}_{A,1} = \mathcal{I}_A \cap \left\{t \in [0, t_1) : g\left(t\right) \geq M_1\right\}$. Then, it follows that $g\left(t\right) < M_1$ for $t \in \mathcal{I}_{A,2}$ but the measure $m\left(\mathcal{I}_{A,2}\right) = 0$, because otherwise, $\operatorname{ess\,inf}\left\{g\left(t\right) : t \in \mathcal{I}_A\right\} < M_1$, contradicting to (24).

On the other hand, for policy $a'\left(t\right)$, partition the active set $\mathcal{I}'_A = \left\{t \in [0, t_1) : g\left(t\right) \geq M_1\right\}$ into two parts, $\mathcal{I}'_A = \mathcal{I}'_{A,1} \cup \mathcal{I}'_{A,2}$, where $\mathcal{I}'_{A,1} = \mathcal{I}'_A \cap \mathcal{I}_A$. It follows that $\mathcal{I}'_{A,2} \subset \mathcal{I}_A^c$, and consequently, $\operatorname{ess\,sup}\left\{g\left(t\right) : t \in \mathcal{I}'_{A,2}\right\} \leq M_2 \leq M_1$ due to (25), while it also holds that $g\left(t\right) \geq M_1$ for $t \in \mathcal{I}'_{A,2}$. This leads to the fact that $g\left(t\right) \equiv M_1$ for $t \in \mathcal{I}'_{A,2}$, formally, $\mathcal{I}'_{A,2} = \{t \in \mathcal{I}_A^c : g\left(t\right) = M_1\}$. Hence, $m\left(\mathcal{I}'_{A,2}\right) = 0$ due to the assumption on zero sojourn time.

To summarize, we have shown that the active sets satisfy $\mathcal{I}_A = (\mathcal{I}_A \cap \mathcal{I}'_A) \cup \mathcal{I}_{A,2}$ and $\mathcal{I}'_A = (\mathcal{I}'_A \cap \mathcal{I}_A) \cup \mathcal{I}'_{A,2}$, where both $\mathcal{I}_{A,2}$ and $\mathcal{I}'_{A,2}$ have measure of 0. This concludes that the optimal policy $a\left(t\right)$ is identical to a threshold policy $a'\left(t\right)$ according to Definition 1. □

APPENDIX C
PROOF OF LEMMA 4

Let $a\left(t\right)$, $t \in [0, t_1)$, be the optimal transmission policy. Recall the definition of $\mathcal{I}_A$, $\mathcal{I}_A^c$, M_1, and M_2, in (23) - (25)

Authorized licensed use limited to: The Chinese University of Hong Kong CUHK(Shenzhen). Downloaded on January 18,2025 at 13:27:52 UTC from IEEE Xplore. Restrictions apply.

in Appendix B. It has been shown that $M_1 \geq M_2$ (Lemma 5). It is clear that when the expected channel sojourn time at $g(t) = M_1$ is zero, then the optimal policy is identical to a threshold policy, according to Lemma 6. Therefore, we focus on the case when the sojourn time is non-zero.

Lemma 7: When the sojourn time $\zeta(M_1)$ is non-zero, then the optimal policy $a(t)$ is an equivalent generalized threshold policy.

Proof: For policy $a(t)$, partition the active set $\mathcal{I}_A$ in (23) into three parts, $\mathcal{I}_A = \mathcal{I}_{A,1} \cup \mathcal{I}_{A,2} \cup \mathcal{I}_{A,3}$, where $\mathcal{I}_{A,1} = \mathcal{I}_A \cap \{t \in [0,t_1) : g(t) > M_1\}$ and $\mathcal{I}_{A,2} = \mathcal{I}_A \cap \{t \in [0,t_1) : g(t) = M_1\}$. Then, it follows that $g(t) < M_1$ for $t \in \mathcal{I}_{A,3}$ and the measure $m(\mathcal{I}_{A,3}) = 0$.

On the other hand, for policy $a'(t)$, partition the active set $\mathcal{I}'_A = \{t \in [0,t_1) : g(t) > M_1\} \cup \{t \in [0,t_1) : g(t) = M_1, t \geq \tau\}$ into three parts, $\mathcal{I}'_A = \mathcal{I}'_{A,1} \cup \mathcal{I}'_{A,2} \cup \mathcal{I}'_{A,3}$, where $\mathcal{I}'_{A,1} = \mathcal{I}_A \cap \{t \in [0,t_1) : g(t) > M_1\}$, $\mathcal{I}'_{A,2} = \{t \in [0,t_1) : g(t) = M_1, t \geq \tau\}$, and $\mathcal{I}'_{A,3} = \mathcal{I}^c_A \cap \{t \in [0,t_1) : g(t) > M_1\}$. Then the measure of interval $\mathcal{I}'_{A,3}$ must be 0 because otherwise $M_2 = \operatorname{ess\,sup}\{g(t) : t \in \mathcal{I}^c_A\} > M_1$, which contradicts to Lemma 5.

Compare the active intervals of two policies, we can find that the measure of sojourn time over states $g(t) > M_1$ are the same, $\mathcal{I}_{A,1} = \mathcal{I}'_{A,1}$, and the time over the interval $\mathcal{I}_{A,3}$ and $\mathcal{I}'_{A,3}$ has on effect on the cost and throughput since $m(\mathcal{I}_{A,3}) = m(\mathcal{I}'_{A,3}) = 0$. Thus if the measure of sojourn time over state $g(t) = M_1$ is the same, policy $a'(t)$ is an equivalent generalized policy of policy $a(t)$. To this end, we set τ such that $m(\mathcal{I}'_{A,2}) = m(\mathcal{I}_{A,2})$, which always has a solution because $m(\mathcal{I}'_{A,2})$ and $m(\mathcal{I}_{A,2})$ have the same range, $(0, \zeta(M_1)]$. □

Appendix D
Proof of Proposition 1 and Proposition 2

A. Proof of Proposition 2

Given η and τ, from the construction of the generalized threshold policies as in (18), denote the active time intervals as

$$\begin{aligned}\mathcal{I}(\eta,\tau) &\triangleq \{t \in [0,t_1) : a(t;\eta,\tau) = 1\} \\ &= \{t \in [0,t_1) : g(t) > \eta\} \cup \{t \in [\tau,t_1) : g(t) = \eta\}.\end{aligned}$$

For $\eta_1 > \eta_2$ and $\tau_1, \tau_2 \in [0,t_1)$, we have the active time intervals

$$\begin{aligned}\mathcal{I}(\eta_1,\tau_1) &\subseteq \{t \in [0,t_1) : g(t) \geq \eta_1\} \\ &\subseteq \{t \in [0,t_1) : g(t) > \eta_2\} \subseteq \mathcal{I}(\eta_2,\tau_2). \qquad (26)\end{aligned}$$

Then, based on the proxy throughput function in (13), we have

$$\tilde{\Upsilon}(\phi_1) = \int_{t \in \mathcal{I}(\eta_1,\tau_1)} c(t)\, dt \leq \int_{t \in \mathcal{I}(\eta_2,\tau_2)} c(t)\, dt = \tilde{\Upsilon}(\phi_2).$$

For $\eta_1 = \eta_2 = \eta$ and $\tau_1 > \tau_2$, we have the active time intervals $\mathcal{I}(\eta_1,\tau_1) \subseteq \mathcal{I}(\eta_2,\tau_2)$ according to (26). Similarly to the above, we have $\tilde{\Upsilon}(\phi_1) \leq \tilde{\Upsilon}(\phi_2)$.

B. Proof of Proposition 1

We first note that there are at most countably many η at which the channel sojourn time $\zeta(\eta) = \int_0^{t_1} \mathbb{I}\{g(t) = \eta\} dt > 0$, because otherwise $\sum_\eta \zeta(\eta) = \infty$ according to [40, P.20], contradicting to the finite transmission duration t_1.

Next, we show that for every (η,τ), $\tilde{\Upsilon}(\phi)$ is either continuous in η or continuous in τ. Moreover, $\tilde{\Upsilon}(\phi)$ is right-continuous in η. Substituting the generalized threshold policy $a(t)$ in (18) to the expression of $\tilde{\Upsilon}(\phi)$ in (13), we have

$$\tilde{\Upsilon}(\phi) = \int_0^{t_1} c(t)\, \mathbb{I}\{g(t) > \eta\}\, dt + \int_\tau^{t_1} c(t)\, \mathbb{I}\{g(t) = \eta\}\, dt \qquad (27)$$

(a) For the continuity in τ, the first term of (27) is independent of τ, and the second term is continuous in τ because its derivative exists as $-c(t)\mathbb{I}\{g(\tau) = \eta\}$. This implies that $\tilde{\Upsilon}(\phi)$ is continuous in τ.

(b) For the continuity in η, since there are at most countably many η_0 such that the channel sojourn time $\zeta(\eta_0) > 0$, for each η_0, there are only two cases: (i) $\int_0^{t_1} \mathbb{I}\{g(t) = \eta\} dt = 0$ for every η in the neighborhood of η_0 or (ii) $\int_0^{t_1} \mathbb{I}\{g(t) = \eta_0\} dt > 0$.

For case (i), the second term in (27) vanishes. Considering $\epsilon > 0$ and $\eta = \eta_0 + \epsilon$, equation (27) becomes

$$\begin{aligned}\tilde{\Upsilon}(\phi(\eta_0,\tau;v,\kappa)) &= \int_0^{t_1} c(t)\, \mathbb{I}\{g(t) > \eta\}\, dt \\ &\quad + \int_0^{t_1} c(t)\, \mathbb{I}\{\eta \geq g(t) > \eta_0\}\, dt \\ &= \tilde{\Upsilon}(\phi(\eta,\tau;v,\kappa)) + H \qquad (28)\end{aligned}$$

where the second term $H \triangleq \int_0^{t_1} c(t)\, \mathbb{I}\{\eta \geq g(t) > \eta_0\}\, dt$ is bounded as

$$\begin{aligned}&\left| \int_0^{t_1} c(t)\, \mathbb{I}\{\eta \geq g(t) > \eta_0\}\, dt \right| \\ &\leq \sup_{0 \leq t < t_1} c(t) \cdot \int_0^{t_1} \mathbb{I}\{\eta_0 + \epsilon \geq g(t) > \eta_0\}\, dt\end{aligned}$$

which converges to 0 as $\epsilon \to 0$. As a result, $\tilde{\Upsilon}(\phi)$ is right-continuous at η_0.

Similarly, we can show that $\tilde{\Upsilon}(\phi)$ is left-continuous at η_0, and hence, $\tilde{\Upsilon}(\phi)$ is continuous at η_0.

For case (ii), there must be $\tilde{\Upsilon}(\phi(\eta_0,0;v,\kappa)) > \tilde{\Upsilon}(\phi(\eta_0,t_1;v,\kappa))$ due to the non-positive derivative on τ and the fact that $\int_0^{t_1} \mathbb{I}\{g(t) = \eta_0\}\, dt > 0$. In addition, consider $\tilde{\Upsilon}(\phi(\eta_0,t_1;v,\kappa))$. The second term in (27) disappears since $\tau = t_1$. As a result, using the same argument in (28), we know that $\tilde{\Upsilon}(\phi(\eta_0,t_1;v,\kappa))$ is right-continuous at η_0.

Due to the continuity of $\tilde{\Upsilon}(\phi)$ and the fact that $\tilde{\Upsilon}(\phi)$ is non-increasing in either η and τ, if (η^*,τ^*) is the optimal solution satisfying $\tilde{\Upsilon}(\phi) > S$, one must find $(\eta',\tau') \neq (\eta^*,\tau^*)$ such that $\tilde{\Upsilon}(\phi^*) > \tilde{\Upsilon}(\phi') > S$, where $\eta' \geq \eta^*$ and $\tau' \geq \tau^*$, with at least one inequality holds strictly. However, in such a case, we can show that $\tilde{E}(\phi^*) > \tilde{E}(\phi')$. To see this,

Authorized licensed use limited to: The Chinese University of Hong Kong CUHK(Shenzhen). Downloaded on January 18,2025 at 13:27:52 UTC from IEEE Xplore. Restrictions apply.

deviating the throughput over (η^*, τ^*) and (η', τ'), we have

$$\begin{aligned}
&\tilde{\Upsilon}(\phi^*) - \tilde{\Upsilon}(\phi') \\
&= \int_{t\in\mathcal{I}(\eta^*,\tau^*)} c(t)\,dt - \int_{t\in\mathcal{I}(\eta',\tau')} c(t)\,dt \\
&= \int_{t\in\mathcal{I}(\eta^*,\tau^*)\setminus\mathcal{I}(\eta',\tau')} c(t)\,dt \\
&\le \sup_{t\in\mathcal{I}(\eta^*,\tau^*)\setminus\mathcal{I}(\eta',\tau')} c(t) \cdot \int_{t\in\mathcal{I}(\eta^*,\tau^*)\setminus\mathcal{I}(\eta',\tau')} dt
\end{aligned}$$

The second equation holds because $\mathcal{I}(\eta', \tau') \subseteq \mathcal{I}(\eta^*, \tau^*)$ according to (26). Since $\tilde{\Upsilon}(\phi^*) > \tilde{\Upsilon}(\phi')$, we have

$$\int_{t\in\mathcal{I}(\eta^*,\tau^*)\setminus\mathcal{I}(\eta',\tau')} dt \ge \frac{\tilde{\Upsilon}(\phi^*) - \tilde{\Upsilon}(\phi')}{\sup_{t\in\mathcal{I}(\eta^*,\tau^*)\setminus\mathcal{I}(\eta',\tau')} c(t)} > 0.$$

Then, based on the energy consumption function in (3), we have

$$\begin{aligned}
\tilde{E}(\phi^*) - \tilde{E}(\phi') &= \int_{t\in\mathcal{I}(\eta^*,\tau^*)\setminus\mathcal{I}(\eta',\tau')} (p(t;\eta,\tau) + \lambda)\,dt \\
&= \int_{t\in\mathcal{I}(\eta^*,\tau^*)\setminus\mathcal{I}(\eta',\tau')} p(t;\eta,\tau)\,dt \\
&\quad + \lambda \int_{t\in\mathcal{I}(\eta^*,\tau^*)\setminus\mathcal{I}(\eta',\tau')} dt
\end{aligned}$$

which is greater than 0. Accordingly, $\tilde{E}(\phi^*) > \tilde{E}(\phi')$, and thus (η^*, τ^*) is strictly sub-optimal, contradicting the hypothesis. In other words, the optimal solution (η^*, τ^*) must satisfies $\tilde{\Upsilon}(\phi) = S$.

Finally, if $g(t)$ is continuous, the equation (26) becomes

$$\begin{aligned}
\mathcal{I}(\eta_1, \tau_1) &\subseteq \{t \in [0, t_1) : g(t) \ge \eta_1\} \\
&\subset \{t \in [0, t_1) : g(t) > \eta_2\} \subseteq \mathcal{I}(\eta_2, \tau_2)
\end{aligned}$$

for any $\eta_1 > \eta_2$, which implies that $m(\mathcal{I}(\eta_2, \tau_2) \setminus \mathcal{I}(\eta_1, \tau_1)) > 0$. Accordingly, for any $\eta_1 > \eta_2$, $\tilde{\Upsilon}(\phi_1) \le \tilde{\Upsilon}(\phi_2)$ holds for all $\tau_1, \tau_2 \in [0, t_1)$. Thus the solution η^* to $\tilde{\Upsilon}(\phi) = S$ is unique.

Appendix E
Proof of Proposition 3

Denote the searching boundaries of η and τ at iteration m and n as $\eta_{\min}^{(m)}$, $\eta_{\max}^{(m)}$ and $\tau_{\min}^{(n)}$, $\tau_{\max}^{(n)}$. It is not difficult to observe that Algorithm 1 always converges because $\left|\eta_{\max}^{(m)} - \eta_{\min}^{(m)}\right|$ and $\left|\tau_{\max}^{(n)} - \tau_{\min}^{(n)}\right|$ both reduce by half at each iteration. Then we will prove the converged result, *i.e.*, the output of Algorithm 1, η^*, τ^*, is the optimal solution to $\mathscr{P}3$.

According to Step 2) in Algorithm 1, for any $m \in \mathbb{Z}^+$, $\tilde{\Upsilon}(\phi(\eta_{\max}^{(m)}, t_1; v, \kappa)) \le S < \tilde{\Upsilon}(\phi(\eta_{\min}^{(m)}, t_1; v, \kappa))$. Denote $\eta^* = \lim_{m\to\infty} \eta_{\max}^{(m)}$, similarly to Appendix D-B, there are only two cases when $\eta = \eta^*$: (i) $\int_0^{t_1} \mathbb{I}\{g(t) = \eta\}\,dt = 0$ for every η in the neighborhood of η^* (case of $\zeta(\eta^*) = 0$) or (ii) $\int_0^{t_1} \mathbb{I}\{g(t) = \eta^*\}\,dt > 0$ (case of $\zeta(\eta^*) > 0$).

For case (i), $\tilde{\Upsilon}(\phi)$ is continuous at η. Thus, when m goes to infinity, $\tilde{\Upsilon}(\phi(\eta_{\max}^{(m)}, t_1; v, \kappa)) = \tilde{\Upsilon}(\phi(\eta_{\min}^{(m)}, t_1; v, \kappa)) = S$. As a result, $\eta^* = \lim_{m\to\infty} \eta_{\max}^{(m)}$, $\tau^* = t_1$ is an optimal solution to $\mathscr{P}3$ according to Proposition 1.

For case (ii), the second bisection search performs, and we have $\tilde{\Upsilon}(\phi(\lim_{m\to\infty} \eta_{\max}^{(m)}, t_1; v, \kappa)) = \tilde{\Upsilon}(\phi(\eta^*, t_1; v, \kappa)) \le S < \tilde{\Upsilon}(\phi(\eta^*, 0; v, \kappa)) = \tilde{\Upsilon}(\phi(\lim_{m\to\infty} \eta_{\min}^{(m)}, t_1; v, \kappa))$. Since $\tilde{\Upsilon}(\phi)$ is continuous at τ, we have that, when n goes to infinity, $\tilde{\Upsilon}(\phi(\eta^*, \tau_{\max}^{(n)}; v, \kappa)) = \tilde{\Upsilon}(\phi(\eta^*, \tau_{\min}^{(n)}; v, \kappa)) = S$. As a result, $\eta^* = \lim_{m\to\infty} \eta_{\max}^{(m)}$, $\tau^* = \lim_{n\to\infty} \tau_{\max}^{(n)}$ is an optimal solution according to Proposition 1.

Appendix F
Proof of Proposition 4

Firstly, we show that game $\mathcal{G}$ is an exact potential game. Given arbitrary $t_k', t_k'' \in \mathcal{T}_k$ and $\boldsymbol{t}_{-k} = \{t_1, t_2, \cdots, t_{k-1}, t_{k+1}, \cdots, t_K\} \in \boldsymbol{\mathcal{T}}_{-k}$, then the deviating value of the function ψ is

$$\begin{aligned}
&\psi(t_k', \boldsymbol{t}_{-k}) - \psi(t_k'', \boldsymbol{t}_{-k}) \\
&= E_{k-1}^*(t_{k-1}, t_k') + E_k^*(t_k', t_{k+1}) + \sum_{i\ne k-1,k} E_i^*(t_i, t_{i+1}) \\
&\quad - E_{k-1}^*(t_{k-1}, t_k'') - E_k^*(t_k'', t_{k+1}) - \sum_{i\ne k-1,k} E_i^*(t_i, t_{i+1}) \\
&= \Lambda_k(t_k', \boldsymbol{t}_{-k}) - \Lambda_k(t_k'', \boldsymbol{t}_{-k}).
\end{aligned}$$

From Definition 2, we have ψ is a potential function of $\mathcal{G}$ and the proposed handover time game $\mathcal{G}$ is an exact potential game.

Then, we prove that there always exists a pure strategy NE for the game $\mathcal{G}$. Firstly, the action space combinations $\boldsymbol{\mathcal{T}}$, the Cartesian product of compact set $\mathcal{T}_k = [t_{k-1}, t_{k+1}]$, is compact. In addition, the potential function $\psi = \sum_{k=0}^{K} E_k^*(t_k, t_{k+1})$ is continuous. This is because, owing to the integral characteristic, similarly to Appendix D-B (a), the objective function (7) and constraint function (8) are continuous with respect to (w.r.t.) t_k and t_{k+1}, and thus the optimal result of (7), $E_k^*(t_k, t_{k+1})$, w.r.t. t_k and t_{k+1} are continuous. Combining the compactness of $\boldsymbol{\mathcal{T}}$ and continuity of ψ, the game $\mathcal{G}$ always has a pure strategy NE according to [38, Theorem 2.3].

Appendix G
Proof of Proposition 5

Suppose that $\boldsymbol{t}^* = (t_1^*, t_2^*, \cdots, t_K^*)$ is a solution to problem $\mathscr{P}1$, *i.e.*, $\psi(\boldsymbol{t}^*) \le \psi(\boldsymbol{t}')$, $\forall \boldsymbol{t}' \in \boldsymbol{\mathcal{T}}$. This leads to $\Lambda_k(t_k^*, \boldsymbol{t}_{-k}^*) \le \Lambda_k(t_k, \boldsymbol{t}_{-k}^*)$, $\forall t_k \in \mathcal{T}_k$, because the change of the Λ_k leads to the exact change of ψ according to Proposition 4. Thus, $\boldsymbol{t}^*$ is an NE of $\mathcal{G}$.

Suppose that $\boldsymbol{t}^* = (t_1^*, t_2^*, \cdots, t_K^*)$ is an NE of $\mathcal{G}$. Thus for all $k \in \mathcal{K}$, there must be $\frac{d}{dt_k}\Lambda_k(t_k, \boldsymbol{t}_{-k})\big|_{t_k=t_k^*} = 0$, because the best response must locate in the stationary points rather than on the boundaries where the utility value is infinity. Thereby, the derivative of the potential function $\frac{d}{d\boldsymbol{t}}\psi$ is

$$\begin{aligned}
\left[\frac{d}{dt_k}\psi\right]_{k\in\mathcal{K}} &= \left[\frac{d}{dt_k}\left(E_{k-1}^*(t_{k-1}, t_k) + E_k^*(t_k, t_{k+1})\right)\right]_{k\in\mathcal{K}} \\
&= \left[\frac{d}{dt_k}\left(\Lambda_k(t_k, \boldsymbol{t}_{-k})\right)\right]_{k\in\mathcal{K}}
\end{aligned}$$

which equals to $\mathbf{0}$ when $\boldsymbol{t} = \boldsymbol{t}^*$. In other words, $\boldsymbol{t}^*$ is a stationary point of $\mathscr{P}1$.

Authorized licensed use limited to: The Chinese University of Hong Kong CUHK(Shenzhen). Downloaded on January 18,2025 at 13:27:52 UTC from IEEE Xplore. Restrictions apply.

APPENDIX H
PROOF OF PROPOSITION 6

Denote the odd-number-node set as $\mathcal{K}_1$, the even-number-node set as $\mathcal{K}_2$, and the strategy sequence generated by the neighbor coordinate response as $\left(\boldsymbol{t}^{(n)}\right)_{n\in\mathbb{Z}^+}$. According to neighbor coordinate response strategy, the response policy can represent as $t_k^{(n+1)} \in \pi_k\left(t_{k-1}^{(n)}, t_{k+1}^{(n)}\right)$ for odd-number node $k \in \mathcal{K}_1$, and as $t_k^{(n+1)} \in \pi_k\left(t_{k-1}^{(n+1)}, t_{k+1}^{(n+1)}\right)$ for even-number node $k \in \mathcal{K}_2$. (The variable $\boldsymbol{t}$ in response function simplifies to $\left\{t_{k-1}, t_{k+1}\right\}$ because only neighbor's strategies, t_{k-1} and t_{k+1}, affect the decision of node k.) This suggests that for an arbitrary nth update, the neighbors will not response simultaneously but in a sequential way, however the nodes in a set can response simultaneously. Since $\mathcal{K}_1$ and $\mathcal{K}_2$ are two independent groups, there is no interdependent update in each set, even though all nodes in one set update simultaneously. In other words, $\Lambda\left(t_k^{(n)}, \boldsymbol{t}_{-k}^{(n)}\right) - \Lambda\left(t_k^{(n-1)}, \boldsymbol{t}_{-k}^{(n-1)}\right) \leq 0, \forall k \in \mathcal{K}$, when better or best response performs. Thus, $\psi\left(\boldsymbol{t}^{(n)}\right) - \psi\left(\boldsymbol{t}^{(n-1)}\right) \leq 0$ according to Proposition 4. (Note that $\psi\left(\boldsymbol{t}^{(n)}\right) - \psi\left(\boldsymbol{t}^{(n-1)}\right) = 0$ iff $\Lambda\left(t_k^{(n)}, \boldsymbol{t}_{-k}^{(n)}\right) - \Lambda\left(t_k^{(n-1)}, \boldsymbol{t}_{-k}^{(n-1)}\right) = 0$ for all nodes, that is, NE achieves.)

In addition, the potential function $\psi(\boldsymbol{t})$ is bounded below, always greater than zero. Thus, there must be $\lim_{n\to\infty} \psi\left(\boldsymbol{t}^{(n)}\right) - \psi\left(\boldsymbol{t}^{(n-1)}\right) = 0$ as well as $\lim_{n\to\infty} \Lambda\left(t_k^{(n)}, \boldsymbol{t}_{-k}^{(n)}\right) - \Lambda\left(t_k^{(n-1)}, \boldsymbol{t}_{-k}^{(n-1)}\right) = 0, \forall k \in \mathcal{K}$. In other words, the neighbor coordinate update with better or best response converges to an NE of game $\mathcal{G}$.

REFERENCES

[1] A. A. Aziz, Y. A. Sekercioglu, P. Fitzpatrick, and M. Ivanovich, "A survey on distributed topology control techniques for extending the lifetime of battery powered wireless sensor networks," *IEEE Commun. Surveys Tuts.*, vol. 15, no. 1, pp. 121–144, 1st Quart., 2013.

[2] N. A. Pantazis, S. A. Nikolidakis, and D. D. Vergados, "Energy-efficient routing protocols in wireless sensor networks: A survey," *IEEE Commun. Surveys Tuts.*, vol. 15, no. 2, pp. 551–591, 2nd Quart., 2013.

[3] F. K. Shaikh and S. Zeadally, "Energy harvesting in wireless sensor networks: A comprehensive review," *Renew. Sustain. Energy Rev.*, vol. 55, pp. 1041–1054, Mar. 2016.

[4] Y. Zeng, R. Zhang, and T. J. Lim, "Wireless communications with unmanned aerial vehicles: Opportunities and challenges," *IEEE Commun. Mag.*, vol. 54, no. 5, pp. 36–42, May 2016.

[5] M. Erdelj, E. Natalizio, K. R. Chowdhury, and I. F. Akyildiz, "Help from the sky: Leveraging UAVs for disaster management," *IEEE Pervasive Comput.*, vol. 16, no. 1, pp. 24–32, Jan. 2017.

[6] N. H. Motlagh, M. Bagaa, and T. Taleb, "UAV-based IoT platform: A crowd surveillance use case," *IEEE Commun. Mag.*, vol. 55, no. 2, pp. 128–134, Feb. 2017.

[7] H. Menouar, I. Guvenc, K. Akkaya, A. S. Uluagac, A. Kadri, and A. Tuncer, "UAV-enabled intelligent transportation systems for the smart city: Applications and challenges," *IEEE Commun. Mag.*, vol. 55, no. 3, pp. 22–28, Mar. 2017.

[8] Y. Zeng, J. Lyu, and R. Zhang, "Cellular-connected UAV: Potential, challenges, and promising technologies," *IEEE Wireless Commun.*, vol. 26, no. 1, pp. 120–127, Feb. 2019.

[9] M. Mozaffari, W. Saad, M. Bennis, Y.-H. Nam, and M. Debbah, "A tutorial on UAVs for wireless networks: Applications, challenges, and open problems," *IEEE Commun. Surveys Tuts.*, vol. 21, no. 3, pp. 2334–2360, 3rd Quart., 2019.

[10] D. Liu et al., "Opportunistic UAV utilization in wireless networks: Motivations, applications, and challenges," *IEEE Commun. Mag.*, vol. 58, no. 5, pp. 62–68, May 2020.

[11] Z. Lin, M. Lin, T. De Cola, J.-B. Wang, W.-P. Zhu, and J. Cheng, "Supporting IoT with rate-splitting multiple access in satellite and aerial-integrated networks," *IEEE Internet Things J.*, vol. 8, no. 14, pp. 11123–11134, Jul. 2021.

[12] R. Levie, Ç. Yapar, G. Kutyniok, and G. Caire, "RadioUNet: Fast radio map estimation with convolutional neural networks," *IEEE Trans. Wireless Commun.*, vol. 20, no. 6, pp. 4001–4015, Jun. 2021.

[13] H. Sun and J. Chen, "Propagation map reconstruction via interpolation assisted matrix completion," *IEEE Trans. Signal Process.*, vol. 70, pp. 6154–6169, 2022.

[14] W. Liu and J. Chen, "UAV-aided radio map construction exploiting environment semantics," *IEEE Trans. Wireless Commun.*, vol. 22, no. 9, pp. 6341–6355, 2023.

[15] J. Zhang, Y. Zeng, and R. Zhang, "UAV-enabled radio access network: Multi-mode communication and trajectory design," *IEEE Trans. Signal Process.*, vol. 66, no. 20, pp. 5269–5284, Oct. 2018.

[16] W. Liu, D. Li, T. Liang, T. Zhang, Z. Lin, and N. Al-Dhahir, "Joint trajectory and scheduling optimization for age of synchronization minimization in UAV-assisted networks with random updates," *IEEE Trans. Commun.*, vol. 71, no. 11, pp. 6633–6646, Nov. 2023.

[17] B. Li, S. Zhao, R. Zhang, and L. Yang, "Full-duplex UAV relaying for multiple user pairs," *IEEE Internet Things J.*, vol. 8, no. 6, pp. 4657–4667, Mar. 2021.

[18] L. Li, T.-H. Chang, and S. Cai, "UAV positioning and power control for two-way wireless relaying," *IEEE Trans. Wireless Commun.*, vol. 19, no. 2, pp. 1008–1024, Feb. 2020.

[19] Q. Hu, Y. Cai, A. Liu, G. Yu, and G. Y. Li, "Low-complexity joint resource allocation and trajectory design for UAV-aided relay networks with the segmented ray-tracing channel model," *IEEE Trans. Wireless Commun.*, vol. 19, no. 9, pp. 6179–6195, Sep. 2020.

[20] F. Cui, Y. Cai, Z. Qin, M. Zhao, and G. Y. Li, "Multiple access for mobile-UAV enabled networks: Joint trajectory design and resource allocation," *IEEE Trans. Commun.*, vol. 67, no. 7, pp. 4980–4994, Jul. 2019.

[21] Q. Hu, Y. Cai, G. Yu, Z. Qin, M. Zhao, and G. Y. Li, "Joint offloading and trajectory design for UAV-enabled mobile edge computing systems," *IEEE Internet Things J.*, vol. 6, no. 2, pp. 1879–1892, Apr. 2019.

[22] C. Shen, T.-H. Chang, J. Gong, Y. Zeng, and R. Zhang, "Multi-UAV interference coordination via joint trajectory and power control," *IEEE Trans. Signal Process.*, vol. 68, pp. 843–858, 2020.

[23] Z. Zhou et al., "When mobile crowd sensing meets UAV: Energy-efficient task assignment and route planning," *IEEE Trans. Commun.*, vol. 66, no. 11, pp. 5526–5538, Nov. 2018.

[24] C. Zhang, L. Zhang, L. Zhu, T. Zhang, Z. Xiao, and X.-G. Xia, "3D deployment of multiple UAV-mounted base stations for UAV communications," *IEEE Trans. Commun.*, vol. 69, no. 4, pp. 2473–2488, Apr. 2021.

[25] Y. Chen, N. Zhao, Z. Ding, and M. Alouini, "Multiple UAVs as relays: Multi-hop single link versus multiple dual-hop links," *IEEE Trans. Wireless Commun.*, vol. 17, no. 9, pp. 6348–6359, Aug. 2018.

[26] B. Li, S. Zhao, R. Zhang, and L. Yang, "Joint transmit power and trajectory optimization for two-way multihop UAV relaying networks," *IEEE Internet Things J.*, vol. 9, no. 23, pp. 24417–24428, Dec. 2022.

[27] S. Zhang, H. Zhang, B. Di, and L. Song, "Cellular UAV-to-X communications: Design and optimization for multi-UAV networks," *IEEE Trans. Wireless Commun.*, vol. 18, no. 2, pp. 1346–1359, Feb. 2019.

[28] C. H. Liu et al., "Energy-efficient UAV control for effective and fair communication coverage: A deep reinforcement learning approach," *IEEE J. Sel. Areas Commun.*, vol. 36, no. 9, pp. 2059–2070, Sep. 2018.

[29] T. Kim and D. Qiao, "Energy-efficient data collection for IoT networks via cooperative multi-hop UAV networks," *IEEE Trans. Veh. Technol.*, vol. 69, no. 11, pp. 13796–13811, Nov. 2020.

[30] S. Fu et al., "Energy-efficient UAV-enabled data collection via wireless charging: A reinforcement learning approach," *IEEE Internet Things J.*, vol. 8, no. 12, pp. 10209–10219, Jun. 2021.

[31] Y. Cui, V. K. N. Lau, R. Wang, H. Huang, and S. Zhang, "A survey on delay-aware resource control for wireless systems—Large deviation theory, stochastic Lyapunov drift, and distributed stochastic learning," *IEEE Trans. Inf. Theory*, vol. 58, no. 3, pp. 1677–1701, Mar. 2012.

[32] B. Li and J. Chen, "Handover game for data transportation over dynamic UAV networks with predictable channels," in *Proc. IEEE Global Commun. Conf.*, Dec. 2022, pp. 3724–3729.

[33] Z. Lin et al., "Refracting RIS-aided hybrid satellite-terrestrial relay networks: Joint beamforming design and optimization," *IEEE Trans. Aerosp. Electron. Syst.*, vol. 58, no. 4, pp. 3717–3724, Aug. 2022.

Authorized licensed use limited to: The Chinese University of Hong Kong CUHK(Shenzhen). Downloaded on January 18,2025 at 13:27:52 UTC from IEEE Xplore. Restrictions apply.

[34] Z. Lin et al., "Pain without gain: Destructive beamforming from a malicious RIS perspective in IoT networks," *IEEE Internet Things J.*, vol. 11, no. 5, pp. 7619–7629, Mar. 2024.

[35] J. A. Fraire, O. De Jonckère, and S. C. Burleigh, "Routing in the space Internet: A contact graph routing tutorial," *J. Netw. Comput. Appl.*, vol. 174, Jan. 2021, Art. no. 102884.

[36] D. Tse and P. Viswanath, *Fundamentals of Wireless Communication*. Cambridge, U.K.: Cambridge Univ. Press, 2005.

[37] D. Fudenberg and J. Tirole, *Game Theory*. Cambridge, MA, USA: MIT Press, 1991.

[38] Q. D. Lã, Y. H. Chew, and B. H. Soong, *Potential Game Theory*. Cham, Switzerland: Springer, 2016.

[39] M. Samir, S. Sharafeddine, C. M. Assi, T. M. Nguyen, and A. Ghrayeb, "UAV trajectory planning for data collection from time-constrained IoT devices," *IEEE Trans. Wireless Commun.*, vol. 19, no. 1, pp. 34–46, Jan. 2020.

[40] G. B. Folland, *Real Analysis: Modern Techniques and Their Applications*. Hoboken, NJ, USA: Wiley, 1984.

Bowen Li (Graduate Student Member, IEEE) received the B.Eng. degree from Harbin Engineering University, Harbin, China, in 2017, and the M.Eng. degree from the University of Chinese Academy of Sciences, China, in 2020. He is currently pursuing the Ph.D. degree with the School of Science and Engineering and the Future Network of Intelligence Institute (FNii), The Chinese University of Hong Kong, Shenzhen (CUHK–Shenzhen), Guangdong, China. His research interests include resource allocation, interference management, network routing, and optimization for wireless communications.

Junting Chen (Member, IEEE) received the B.Sc. degree in electronic engineering from Nanjing University, Nanjing, China, in 2009, and the Ph.D. degree in electronic and computer engineering from The Hong Kong University of Science and Technology (HKUST), Hong Kong, SAR, China, in 2015.

From 2014 to 2015, he was a Visiting Student with the Wireless Information and Network Sciences Laboratory, MIT, Cambridge, MA, USA. He is currently an Assistant Professor with the School of Science and Engineering and the Future Network of Intelligence Institute (FNii), The Chinese University of Hong Kong, Shenzhen (CUHK–Shenzhen), Guangdong, China. Prior to joining CUHK–Shenzhen, he was a Post-Doctoral Research Associate with the Ming Hsieh Department of Electrical Engineering, University of Southern California (USC), Los Angeles, CA, USA, from 2016 to 2018, and with the Communication Systems Department, EURECOM, Sophia–Antipolis, France, from 2015 to 2016. His research interests include channel estimation, MIMO beamforming, machine learning, and optimization for wireless communications and localization. His current research interests include radio map sensing, construction, and application for wireless communications. He was a recipient of the HKTIIT Post-Graduate Excellence Scholarships in 2012. He was nominated as the Exemplary Reviewer of IEEE WIRELESS COMMUNICATIONS LETTERS in 2018. His paper received the Charles Kao Best Paper Award from WOCC 2022.

Authorized licensed use limited to: The Chinese University of Hong Kong CUHK(Shenzhen). Downloaded on January 18,2025 at 13:27:52 UTC from IEEE Xplore. Restrictions apply.